Asteroids *Do* Have Satellites

William J. Merline
Southwest Research Institute

Stuart J. Weidenschilling
Planetary Science Institute

Daniel D. Durda
Southwest Research Institute

Jean-Luc Margot
California Institute of Technology

Petr Pravec
*Astronomical Institute of the Academy of Sciences
of the Czech Republic*

Alex D. Storrs
Towson University

After years of speculation, satellites of asteroids have now been shown definitively to exist. Asteroid satellites are important in at least two ways: (1) They are a natural laboratory in which to study collisions, a ubiquitous and critically important process in the formation and evolution of the asteroids and in shaping much of the solar system, and (2) their presence allows to us to determine the density of the primary asteroid, something which otherwise (except for certain large asteroids that may have measurable gravitational influence on, e.g., Mars) would require a spacecraft flyby, orbital mission, or sample return. Binaries have now been detected in a variety of dynamical populations, including near-Earth, main-belt, outer main-belt, Trojan, and transneptunian regions. Detection of these new systems has been the result of improved observational techniques, including adaptive optics on large telescopes, radar, direct imaging, advanced lightcurve analysis, and spacecraft imaging. Systematics and differences among the observed systems give clues to the formation mechanisms. We describe several processes that may result in binary systems, all of which involve collisions of one type or another, either physical or gravitational. Several mechanisms will likely be required to explain the observations.

1. INTRODUCTION

1.1. Overview

Discovery and study of small satellites of asteroids or double asteroids can yield valuable information about the intrinsic properties of asteroids themselves as well as their history and evolution. Determination of orbits of these moons can provide precise determination of the total (primary + secondary) mass of the system. In the case of a small secondary, the total mass is dominated by the primary. For a binary with a determinable size ratio of components (e.g., double asteroids), an assumption of similar densities can yield individual masses. If the actual sizes of the primary or the pair are also known, then reliable estimates of the primary's bulk density — a fundamental property — can be made. This reveals much about the composition and structure of the primary and will allow us to make comparisons between, for example, asteroid taxonomic types and our inventory of meteorites. In general, uncertainties in the asteroid size will dominate the uncertainty in density. We define satellites to be small secondaries, a double asteroid to be a system with components of similar size, and a binary to be any two-component system, regardless of size ratio.

Similarities and differences among the detected systems reveal important clues about possible formation mechanisms. Systematics are already being seen among the main-belt binaries; many of them are C-like and several are family members. There are several theories to explain the origin of these binary systems, all of them involving disruption of the parent object, either by physical collision or gravitational interaction during a close pass to a planet. It is likely that several of the mechanisms will be required to explain the observations.

The presence of a satellite provides a real-life laboratory to study the outcome of collisions and gravitational inter-

actions. The current population probably reflects a steady-state process of creation and destruction. The nature and prevalence of these systems will therefore help us understand the collisional environment in which they formed and will have further implications for the role of collisions in shaping our solar system. They will also provide clues to the dynamical history and evolution of the asteroids.

A decade ago, binary asteroids were mostly a theoretical curiosity, despite sporadic unconfirmed satellite detections. In 1993, the *Galileo* spacecraft made the first undeniable detection of an asteroid moon with the discovery of Dactyl, a small moon of Ida. Since that time, and particularly in the last year, the number of known binaries has risen dramatically. In the mid to late 1990s, the lightcurves of several near-Earth asteroids (NEAs) revealed a high likelihood of being binary. Previously odd-shaped and lobate NEAs, observed by radar, have given way to signatures revealing that at least six NEAs are binary systems. These lightcurve and radar observations indicate that among the NEAs, the binary frequency may be ~16% (see sections 2.4 and 2.5).

Among the main-belt asteroids, we now know of eight confirmed binary systems, although the overall frequency of these systems is likely to be low, perhaps a few percent (see section 2.2.6). These detections have come about largely because of significant advances in adaptive-optics systems on large telescopes, which can now reduce the blurring of the Earth's atmosphere to compete with the spatial resolution of space-based imaging [which is also, via the Hubble Space Telescope (HST), now contributing valuable observations]. Searches among the Trojans and transneptunian objects (TNOs) have shown that other dynamical populations also harbor binaries.

With new reliable techniques for detection, the scientific community has been rewarded with many examples of systems for study. This has in turn spurred new theoretical thinking and numerical simulations, techniques for which have also improved substantially in recent years.

1.2. History and Inventory of Binary Asteroids

Searches for satellites can be traced back to William Herschel in 1802, soon after the discovery of the first asteroid, (1) Ceres. The first suspicion of an asteroidal satellite goes back to *Andre* (1901), who speculated that the β-Lyrae-like lightcurve of Eros could result from an eclipsing binary system. Of course, we now know definitively that this interpretation is wrong (*Merline et al.,* 2001c), Eros being one of the few asteroids visited directly by spacecraft (cf. *Cheng,* 2002).

The late 1970s saw a flurry of reports of asteroid satellites, inferred from indirect evidence, such as anomalous lightcurves or spurious secondary blinkouts during occultations of stars by asteroids. *Van Flandern et al.* (1979) in *Asteroids* give a complete summary of the evidence at that time. To some, the evidence was highly suggestive that satellites were common. To date, however, none of those suspected binaries has been shown to be real, despite rather intensive study with modern techniques.

In the 1980s, additional lines of evidence were pursued, including asteroids with slow rotation, asteroids with fast rotation, and the existence of doublet craters on, e.g., the Moon or Earth. *Cellino et al.* (1985) studied 10 asteroids that showed anomalous lightcurves, which they compared with predictions from models of equilibrium binaries of varying mass ratios by *Leone et al.* (1984). Model separations and magnitude differences for these putative binaries were given; most of these could have been detected using modern observations, but none have been confirmed as separated binaries, although *Ostro et al.* (2000a), *Merline et al.* (2000b), and *Tanga et al.* (2001) have shown (216) Kleopatra to be a contact binary. In the same decade, radar emerged as a technique capable of enabling study of a small number of (generally nearby) asteroids. In addition, speckle interferometry was used to search for close-in binaries, and the advent of CCD technology allowed for more sensitive and detailed searches. Studies by *Gehrels et al.* (1987), who searched 11 main-belt asteroids using direct CCD imaging and by *Gradie and Flynn* (1988), who searched 17 main-belt asteroids, using a CCD/coronagraphic technique, did not produce any detections. By the end of the decade, previous optimism about the prevalence of satellites had retreated to claims ranging from their being essentially nonexistent (*Gehrels et al.,* 1987) to their being rare (*Weidenschilling et al.,* 1989). *Weidenschilling et al.* (1989) give a summary of the status of the observations and theory at the time of *Asteroids II*.

The tide turned in 1993, when the *Galileo* spacecraft, en route to its orbital tour of the Jupiter system, flew past (243) Ida and serendipitously imaged a small (1.4-km-diameter Dactyl) moon orbiting this 31-km-diameter, S-type asteroid. This discovery spurred new observations and theoretical thinking on the formation and prevalence of asteroid satellites. *Roberts et al.* (1995) performed a search of 57 asteroids, over multiple observing sessions, using speckle interferometry. No companions were found in this survey. A search by *Storrs et al.* (1999a) of 10 asteroids using HST also revealed no binaries. Numerical simulations performed by *Durda* (1996) and *Doressoundiram et al.* (1997) showed that the formation of small satellites may be a fairly common outcome of catastrophic collisions. *Bottke and Melosh* (1996a,b) suggest that a sizable fraction (~15%) of Earth-crossing asteroids may have satellites, based on their simulations and the occurrence of doublet craters on Earth and Venus. Various theoretical studies have been performed on the dynamics and stability of orbits about irregularly shaped asteroids (*Chauvineau and Mignard,* 1990; *Hamilton and Burns,* 1991; *Chauvineau et al.,* 1993; *Scheeres,* 1994).

After the first imaging of an asteroid moon by *Galileo,* several reports of binaries among the NEA population, based on lightcurve shapes, were made by Pravec et al. and Mottola et al., including 1994 AW$_1$ (*Pravec and Hahn,* 1997), 1991 VH (*Pravec et al.,* 1998a), 3671 Dionysus (*Mottola*

et al., 1997), and 1996 FG$_3$ (*Pravec et al.,* 1998b). While these systems are likely to be real, they have not been confirmed by direct imaging or radar techniques.

It was not until 1998 that the first definitive and verifiable evidence for an asteroid satellite was acquired from Earth, when 215-km (45) Eugenia was found to have a small moon (13-km Petit Prince) by direct imaging assisted by adaptive optics (AO) (*Merline et al.,* 1999b,c). This discovery was the first result from a dedicated survey with the capability to search for faint companions (Δm ~ 7 mag) as close as a few tenths of an arcsecond from the primary. This survey detected two more asteroid binaries in 2000: (762) Pulcova (*Merline et al.,* 2000a) and (90) Antiope (*Merline et al.,* 2000a,b). While the moon of Pulcova is small, Antiope is truly a double asteroid, with components of nearly the same size.

After these detections, the first two NEA binaries to be definitively detected by radar were announced: 2000 DP$_{107}$ (*Ostro et al.,* 2000b; *Margot et al.,* 2000) and 2000 UG$_{11}$ (*Nolan et al.,* 2000). In the meantime, Pravec and colleagues have continued to add to the rapidly growing list of suspected binary NEAs from lightcurves.

Starting in 2001, the discovery of binary discoveries really surged. In February, *Brown and Margot* (2001), also using adaptive-optics technology, discovered a moon of (87) Sylvia, a Cybele asteroid beyond the main belt. Soon afterward, *Storrs et al.* (2001a) reported a moon of (107) Camilla, also a Cybele, using HST observations. Four additional radar binaries were announced: 1999 KW$_4$ (*Benner et al.,* 2001a), 1998 ST$_{27}$ (*Benner et al.,* 2001b), 2002 BM$_{26}$ (*Nolan et al.,* 2002a), and 2002 KK$_8$ (*Nolan et al.,* 2002b). In addition, *Veillet et al.* (2001, 2002) reported the first binary among transneptunian objects (aside from Pluto/Charon), 1998 WW$_{31}$, obtained by direct CCD imaging without AO. Six more TNO doubles were reported: 2001 QT$_{297}$ (*Eliot et al.,* 2001); 2001 QW$_{322}$ (*Kavelaars et al.,* 2001); 1999 TC$_{36}$ (*Trujillo and Brown,* 2002); 1998 SM$_{165}$ (*Brown and Trujillo,* 2002); 1997 CQ$_{29}$ (*Noll et al.,* 2002a); and 2000 CF$_{105}$ (*Noll et al.,* 2002b). A small moon was discovered around (22) Kalliope by *Margot and Brown* (2001) and *Merline et al.* (2001a); this was the first M-type asteroid known to have a companion. Later, the first binary Trojan asteroid, (617) Patroclus, was found (*Merline et al.,* 2001b); this asteroid, like Antiope, has components of nearly equal size. *Merline et al.* (2002) then detected a widely spaced binary in the main belt, (3749) Balam, which appears to be the most loosely bound system known. (The list of asteroid satellites in this chapter is complete as of August 2002.)

1.3. Observational Challenges

Direct imaging of possible satellites of asteroids has been hampered by the lack of adequate angular resolution to distinguish objects separated by fractions of an arcsecond and by the lack of sufficient dynamic range of detectors to resolve differences in brightness of many magnitudes. The basic observational problem, detection of a faint object in close proximity to a much brighter one, is common to many areas of astronomy, such as binary and multiple star systems or circumstellar and protostellar disks.

At the inner limit, the smallest separations between the primary asteroid and the companion are determined by orbital instabilities (a few radii of the primary); at the far extreme, they are determined by the Hill stability limit (a few hundred radii of the primary for the main belt). For a 50-km-diameter main-belt asteroid (say at 2.5 AU), observed at opposition, the angular separation at which we might find a satellite spans the range of ~0.05 arcsec to several arcsec. If the satellite has a diameter of 2 km, the brightness difference is 7 mag. Using conventional telescopes, the overlapping point-spread functions of these objects of widely disparate brightness make satellite detection in the near field extraordinarily challenging. The FWHM of the uncorrected point spread function of a large groundbased telescope, under average seeing conditions of 1 arcsec, corresponds to nearly 25 primary radii in the above example. Indeed, both theory and most examples of observed binaries suggest that moons are more likely to be found closer to the primary.

The traditional detection techniques have been deep imaging using multiple short exposures to search the nearfield and the use of "coronagraphic" cameras for the farfield. With modern, low-noise, high-dynamic-range detectors and with the advent of adaptive-optics technology, a ground-based search for and study of, asteroid satellites has been realized.

Radar is a powerful technique for nearby objects because the return signal is proportional to the inverse 4th power of the distance. This has limited study to either very large asteroids at the inner edge of the main belt or to NEAs. Radar has shown tremendous promise and upgrades to the telescopes and electronics have enhanced the range and capabilities. Observations of NEAs, however, have drawbacks because the objects are small and opportunities to observe them may be spaced many years apart. Therefore, it is difficult to make repeat or different observations.

Lightcurve observations generally require the observed system to be nonsynchronous, i.e., having a primary rotation rate different from the orbital rate. In addition, either the system must be eclipsing or the secondary must have an elongated shape. Such a system will show a two-component lightcurve. To be well resolved, both contributions should have an amplitude of at least a few hundredths of a magnitude. The requirements generally restrict efficient observations to close-in binary systems with the secondary's diameter at least approximately one-fifth that of the primary. This technique works best also on NEAs, where these small binaries appear to have a long tidal evolution timescale and therefore can remain nonsynchronous for a long time after formation. These close binaries also lend themselves to having a high probability of eclipse at any given time. This technique suffers from the same problems with NEAs men-

tioned above: Relatively quick repeat observations over a wide range of viewing geometries are not possible. Thus, in many cases there may be ambiguities in interpretation of the lightcurve signatures.

Direct imaging has been shown to be possible for TNOs because those detected so far have wide separations and large secondary/primary size ratios. So although these objects are far away (~45 AU), loosely bound binaries can be separated with conventional (non-AO) imaging under ideal conditions. HST searches for main-belt binaries have been largely unsuccessful, not because of limitations to instrumentation, but because of the lack of telescope time allocated. HST searches for TNO binaries are now under way and are showing promising results.

2.   OBSERVATIONAL TECHNIQUES AND DISCOVERIES

2.1.   Searches During Spacecraft Encounters

One of the most effective ways of performing a search for satellites of asteroids is by a flyby or orbital tour with a spacecraft, although this is prohibitively expensive for more than a few objects. Nonetheless, this method produced the first definitive evidence for the existence of asteroid moons. It also allows searches to much smaller sizes than is possible from Earth.

A variety of problems are encountered when searching for satellites in images taken during spacecraft encounters. A major problem is that the images are taken from a rapidly moving platform. This makes quick visual inspection difficult, because one must project the image to a common reference point. If the moon is resolved, as in the case of Dactyl, the problem is more manageable. But it is possible that moons would appear as small, pointlike objects, competing for recognition with stars, cosmic-ray hits, and detector defects. The strategy is normally to take a series of many pictures, in which the detector defects are known and the cosmic rays may be eliminated through lack of persistence. Stars may be eliminated by identification using star catalogs or by common motion. Even with these techniques, however, cosmic-ray hits in a series of images may conspire to cluster in a pattern consistent with the spacecraft motion and an object in a plausible position in three-dimensional space relative to the asteroid. Correlations among all identified point-source candidates on a series of images must be examined.

2.1.1.   Discovery of Dactyl.   The first image of an asteroid moon was spotted by Ann Harch of the *Galileo* Imaging Team on February 17, 1994, during playback of images from *Galileo*'s encounter with S-type (243) Ida on August 29, 1993. Because of the loss early in the mission of *Galileo*'s high-gain antenna, some data from the Ida encounter were returned months afterward. The first images were returned as "jailbars," or thin strips of a few lines of data separated by gaps. This technique allowed a quick look at the contents of the images to determine which lines contained Ida data. Fortuitously, one of these lines passed through the satellite,
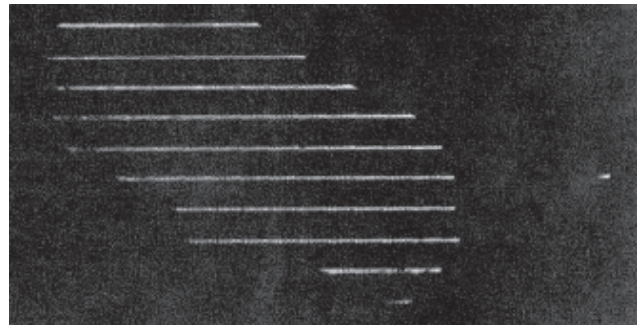

Fig. 1.   Discovery image for Dactyl, the first known asteroid satellite (*Belton et al.,* 1996). It was taken by *Galileo* on August 29, 1993, from a range of 10,719 km. The picture has a resolution of ~100 m/pixel. Because of limited downlink, not all images could be returned. Instead, this technique of playing back image strips was used to find the relevant images or portions of images that contained Ida. The resulting "jailbar" image here fortuitously provides the first clue of an extended object, with the expected photometric profile, off the bright limb of Ida.

as shown in Fig. 1. The presence of the moon was later confirmed by the infrared spectrometer experiment and was announced by *Belton and Carlson* (1994). It was initially dubbed 1993(243)1, as the first satellite of asteroid (243) to be discovered in 1993, and was later given the permanent name Dactyl, after the Dactyli, the children or protectors of Ida.

During the flyby of Ida, 47 images of Dactyl were obtained (*Chapman et al.,* 1995; *Belton et al.,* 1995, 1996). However, because there was no opportunity for feedback to guide an imaging sequence, these pictures were all serendipitous. The spacecraft trajectory was nearly in the plane of the satellite motion, and hence little relative motion was observed, resulting in poorly determined orbital parameters. Followup observations with HST (*Belton et al.,* 1995, 1996) failed to find the satellite, which was not surprising given its separation. But if the object were on a hyperbolic or highly elliptical orbit, there would be some chance of finding it with HST. These additional observations did allow limits to be set on the density of Ida.

Additionally, resolved pictures of Dactyl's surface have allowed for geological interpretation and have provided a glimpse into the possible origin and history of an asteroid moon. The pair is shown in Fig. 2, with a smaller-scale image of Dactyl in Fig. 3. *Chapman et al.* (1996) and *Veverka et al.* (1996b) indicate that the crater size-frequency distribution on both Ida and Dactyl exhibit equilibrium saturation (see also *Chapman,* 2002). Thus, we can estimate only the minimum ages for both objects; the relative age of the two, from crater data alone, is uncertain. Given the observed impactor size-distribution, saturation at the largest craters on Ida, ~10 km, would be expected after about 2 b.y. (*Chapman et al.,* 1996), setting roughly the minimum age of Ida. The largest craters on Dactyl, however, are less than 0.4 km in size, and would saturate in about 30 m.y. Impacts that would create larger craters on Dactyl would instead break
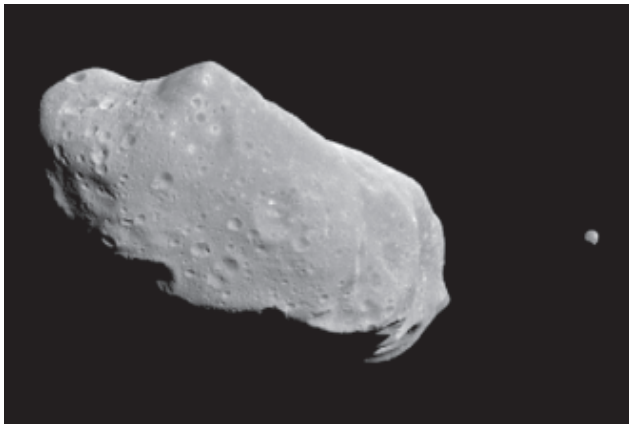
Fig. 2. Full image of Ida and Dactyl, taken from approximately the same range and with the same resolution listed in Fig. 1. The picture is in a green filter. Ida is ~56 km long and Dactyl is roughly spherical with a diameter of ~1.4 km. At this time Dactyl is in the foreground, ~85 km (5.5 R_{Ida}) from Ida's center, and moving at about 6 m s^{-1}. The orbit is prograde with respect to Ida's spin, which itself is retrograde with respect to the ecliptic.

up the object. The mean time between impacts that would destroy Dactyl is estimated by *Davis et al.* (1996) to be, depending on model assumptions, between about 3 m.y. and 240 m.y., the same order as the saturation cratering age. If Dactyl was formed 2 b.y. ago with Ida, via disruptive capture (section 3.3), perhaps during the Koronis-family breakup (*Binzel,* 1988), then it is very unlikely that it would still exist intact, given its short lifetime against collisional breakup. Conceivably, it may have formed from the ejecta of a more recent, large cratering event (section 3.2). Either way, it must have been disrupted and reaccreted several times since

Fig. 3. Highest-resolution picture of Dactyl, at 39 m/pixel, showing shape and surface geology. The topography is dominated by impact craters, without prominent grooves or ridges.

its initial formation, because it is unlikely to have formed only in the last 30 m.y. Additional geological data support the idea of this satellite as a reaccumulated rubble pile. It is roughly spherical, with no obvious evidence of coherent monolithic structure. It displays a softened appearance and likely has a surface regolith (*Veverka et al.,* 1996b).

The spectrum of Dactyl (from *Galileo* imager data, 0.4–1.0 µm) is similar to that of Ida (*Veverka et al.,* 1996a), but with some important differences. Both objects show S-type spectra and have similar albedos. Dactyl, however, shows somewhat less reddening than Ida, possibly indicating less space weathering, which is also consistent with a younger surface age, as expected from the most recent disruption/reaccretion episode (*Chapman,* 1996).

2.1.2. Other searches. Extensive searches were made for additional satellites of Ida in the *Galileo* datasets; no candidates were found that were not consistent with single or multiple cosmic-ray events (*Belton et al.,* 1995, 1996). The searches were made at spacecraft-to-asteroid ranges of 200,000 km (satellite-detection size limit ~800 m), 10,000 km (size limit ~50 m), and 2400 km (encounter; size limit ~10 m).

Cursory searches for satellites were made during the *Galileo* flyby of S-type (951) Gaspra in 1991, with no detections of objects larger than 27 m out to ~10 Gaspra radii (*Belton et al.,* 1992).

The *NEAR Shoemaker* spacecraft made a fast flyby of C-type, inner main-belt asteroid (253) Mathilde in 1997 en route to its orbital encounter with (433) Eros. A well-planned imaging sequence to search for satellites was performed and a thorough search made (*Merline et al.,* 1998; *Veverka et al.,* 1999a). More than 200 images were taken specifically to search for satellites. No unambiguous evidence for satellites larger than 40 m diameter was found within the searchable volume, which was estimated to be ~4% of the Hill sphere. The portion, however, of the Hill sphere searched was an important one, inside roughly 20 radii of Mathilde (almost all of the known main-belt binaries show separations well below 20 primary radii). From approach images, which were less sensitive due to lighting geometry, no satellites larger than 10 km were found in the entire Hill sphere.

The *NEAR Shoemaker* spacecraft continued on to an unplanned flyby of (433) Eros, an S-type NEA, in December 1998 (cf. *Cheng,* 2002). The first critical burn of the main rocket for the rendezvous aborted prematurely, which led to execution of a contingency imaging sequence. This included a search for satellites down about 50 m in the entire Hill sphere (*Merline et al.,* 1999a; *Veverka et al.,* 1999b). About one year later, after engineers had diagnosed the problem and brought the spacecraft slowly back to Eros, the orbital tour of Eros began. During approach to orbit insertion, another, more detailed and thorough search for satellites was made. During this search, both manual and automated searches were performed (*Merline et al.,* 2001c; *Veverka et al.,* 2000). This was the first systematic search for satellites of the entire Hill sphere of an asteroid down to small sizes. The search found no objects at diameter 20 m (95% confidence) and none at 10 m (with 70% confidence).

2.2. Adaptive Optics on Large Groundbased Telescopes

Given the observational challenges just discussed and the number of failed attempts to detect asteroid satellites, it was clear that a new approach was needed. In 1996, Merline and collaborators began to apply a relatively new technology in hopes of achieving high-contrast, high-spatial-resolution imaging on a large number of targets from groundbased telescopes. This new technique, called adaptive optics (AO), ultimately led to the first Earth-based images of satellites.

2.2.1. Method and capabilities. This technique minimizes the distortion in an astronomical image by sensing and correcting, in real time, aberrations due to the Earth's atmosphere, usually by means of a deformable mirror. This new technology can result in diffraction-limited imaging with the largest groundbased telescopes. Compared with conventional direct-imaging techniques, this technique shows a dramatic improvement in the ability to detect asteroid companions. Adaptive optics (1) decreases the light contribution from the primary asteroid at the position of the satellite on the plane of the sky and (2) increases the signal from the secondary asteroid at that position, enhancing the ability to detect, or set limits on the sizes of, satellites. In addition, because IR-imaging cameras are used, no charge bleeding (as for CCDs) occurs in an overexposure of the primary. This effectively gives near-field coronagraphic imaging capability, allowing deep exposures for faint companions.

In adaptive-optics systems, the light from the telescope is processed by a separate optical unit that resides beyond the telescope focal plane. A recollimated beam impinges on a deformable mirror (DM), which has many actuators that can be adjusted rapidly to "correct" the beam back to its undistorted "shape." Light from the DM is then divided, with part (typically near-IR) of it going to the science camera, and part (typically visible) going to a wavefront sensor, which analyzes the deformation of the wavefront and provides correction signals to the DM, forming a closed loop.

Two types of systems are in use. One uses a Shack-Hartmann (SH) wavefront sensor, basically an x-y array of many lenslets in a collimated beam. Each of these lenslets allows sensing of the beam deviation in a different part of the pupil. The other method is curvature-wavefront sensing (CS) (*Roddier,* 1988) in which the wavefront sensor is divided in a radial/sectoral fashion. The illumination pattern of the beam is then sampled rapidly at positions on either side of a focal plane; the differences in illumination are related to the local wavefront curvature. While the Shack-Hartmann systems are more common, the curvature systems can work with fewer elements, at faster speeds, and on fainter objects. CS systems trade the higher-order corrections of an SH system for faster (kHz) sample and correction speeds.

There are many AO systems either in use or under development. Among those that have been used for planetary applications are systems at the Starfire Optical Range (U.S. Air Force), the Mt. Wilson 100", the University of Hawai'i (on 88", UKIRT, and CFHT), the Canada-France-Hawai'i Telescope (CFHT), the Keck, the ESO/Adonis, the Lick, the Palomar, and the Gemini North. Only three of these systems, all located on Mauna Kea, Hawai'i, have resulted in discoveries of asteroid satellites. The 3.6-m CFHT uses a 19-element CS system called PUEO (*Roddier et al.,* 1991; *Rigaut et al.,* 1998). It can reach a limiting magnitude of about V = 14.5 with a resolution of about 0.11 arcsec at H-band. The 10-m Keck uses a 349-element SH system (*Wizinowich et al.,* 2000), allowing compensation to about V = 13 with a resolution of 0.04 arcsec at H-band. The 8.1-m Gemini telescope, with the Hokupa'a 36-element CS system (*Graves et al.,* 1998) of the University of Hawai'i, can reach about V = 17.5, with resolution of ~0.05 arcsec at H-band.

The AO systems must have a reference point source to compute atmospheric turbulence. The systems may either use a natural guide star (NGS) or an artificially generated star (LGS), in which a laser is used to produce a point source in the upper atmosphere. Laser-guide systems have been tested and used largely within military applications. Although there are plans for LGS systems at many astronomical facilities, the progress has been slow and of limited use thus far. Therefore, NGS systems dominate AO systems. For astronomical (fixed-source) applications, a nearby brighter star may be used, provided it is within the isoplanatic patch, which may be about 20 arcsec at 2 μm. But for planetary objects, e.g., main-belt asteroids, their fast motion prohibits use of nearby objects, and one must rely on the object itself as the reference. This presents two limitations: Extended objects will tend to degrade the quality of the compensation, although asteroids are not extended enough to be of concern. In addition, the quality of the AO correction will depend on the brightness of the reference object, so there is a limit to how faint an asteroid can be observed.

Most of the AO systems operate in the near IR, using HgCdTe IR (1–2.5 μm) array detectors as the science camera. Although the ultimate signal-to-noise of the science data is a function of the brightness in the selected IR band, it is the visible light that is used by the wavefront sensor, so the quality of the AO compensation is dependent upon the V magnitude.

The correct wavelength band for observations is adjusted depending on conditions and the telescope. With IR AO observations, there is always a tradeoff between competing effects — the shorter the wavelength, the narrower the PSF for a given telescope. But at shorter wavelengths, the number of cells in the telescope beam that need to be continuously corrected grows beyond the capacity of the AO system — more cells require more AO actuators for compensation. But systems with a large number of actuators means prohibitively high cost, so there is a limit. Of course, the larger the telescope, the larger the number of cells needed to compensate. Therefore, the 10-m Keck usually performs best at K'-band (2.1 μm) and the 3.6-m CFHT at H-band (1.6 μm). Thus, the Strehl ratio (the ratio of peak brightness of acquired image to the peak brightness of a perfectly diffraction-limited point source) increases at longer wave-

lengths, while the instrumental width also increases. Under good conditions one hopes to achieve about 50% Strehl. On exceptionally good nights, it may be possible to use J-band (1.2 μm) for a narrower PSF.

The future holds great promise for AO, as more telescopes adopt this technology. In addition, the advent of quality LGS systems and the opportunity for systems employing many more actuators, as costs decline and computer speeds increase, means the possibility of visible-light systems and a correspondingly narrower diffraction limit.

Using AO, because the result is a picture of the system on the plane of the sky, we can hope to achieve the same information (and more) about a system as that which can be obtained from visual binary stars, only on a substantially shorter timescale. Basically, all seven dynamic orbital elements required to describe the motion are derivable. These are the elements describing motion along the orbital ellipse — the semimajor axis, the eccentricity, and an indication of orbital phase, such as time of periapse passage or true anomaly — plus the elements describing the orientation in three-dimensional space — e.g., the inclination, the longitude of the ascending node, and the argument of periapse. In addition, because the system mass is unknown (unlike Sun-orbiting objects) we also require determination of the orbital period. From a limited span of observations, say a single orbit or series of a few orbits, there remains a two-fold ambiguity in the orbital pole position (determination of the pole direction is equivalent to determination of the two elements inclination and node). This can be resolved by observing at a different viewing geometry at some later time. The period and orbit size (assuming a circular orbit) are readily obtainable, which immediately yields an estimate of the system (primary + secondary) mass, by Kepler's Third Law. If the secondary is small or if we can independently determine the size ratio (and then make an assumption that the primary and secondary are of the same density), then the primary mass can be estimated. If the primary asteroid size is known, then we can determine the primary's density. Of course, density is clearly one of the most fundamental parameters one hopes to know about any body, and gives direct insight into the composition and structure. Because most of the orbits are small in angular terms (and pixels on a detector), the errors in measurement of positions translate into sizable uncertainties in most of the orbital elements. However, the period can be very accurately determined, and the ultimate uncertainties in density are dominated by uncertainties in the size of the asteroid.

2.2.2. (45) Eugenia. The first binary system discovery using AO was accomplished on November 1, 1998, when a small companion of (45) Eugenia was discovered at the CFHT by *Merline et al.* (1999b,c). The system was tracked for 10 d and again occasionally in the following months and years. It was the first AO system for which the two-fold degeneracy in the orbit pole had been resolved. Further, because of the large brightness difference (about 7 mag), it remains one of the more difficult AO binaries to observe. Figure 4 shows the discovery image of this object, provisionally named S/1998 (45) 1 and later given the permanent
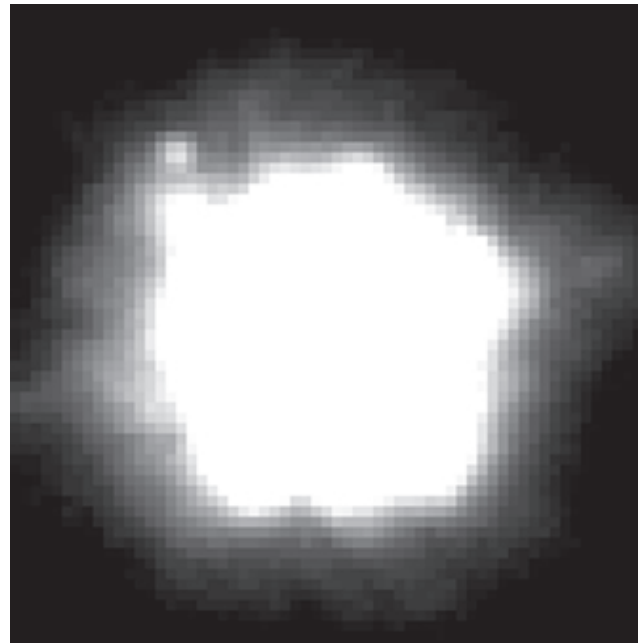

Fig. 4. Discovery image of Petit Prince, moon of (45) Eugenia, taken at the Canada-France-Hawai'i Telescope on November 1, 1998, using the PUEO adaptive-optics system (*Merline et al.,* 1999b). It is the first asteroid moon to be imaged from Earth. The image is an average of 16 images of exposure 15 s. It is taken in H-band (1.65 μm) and has a plate scale of 0.035 arcsec/pixel. The separation of the moon is ~0.75 arcsec from Eugenia and has a brightness ratio of ~7 mag.

name Petit Prince in honor of the prince imperial of France, the only child of Napoleon III and his wife Empress Eugenie (namesake of Eugenia). (The name itself is derived from the popular children's book *Le Petit Prince* by A. Saint-Exupery, whose central character was an asteroid-dwelling Little Prince.) The intention was to keep and solidify the tradition of naming asteroid moons after the children or other derivative of the parent asteroid. Figure 5 shows five epochs of the orbit at the time of discovery. Figure 6 exhibits the tremendous power of modern AO techniques both to resolve the asteroid and to clearly separate a close companion.

The satellite appears to be roughly in the asteroid's equatorial plane and in a prograde orbit (*Merline et al.,* 1999c). A prograde orbit is preferred for a satellite formed from impact-generated orbital debris (*Weidenschilling et al.,* 1989; *Durda and Geissler,* 1996). A retrograde orbit, however, is more stable against perturbing effects of the nonuniform gravitational field of an oblate primary (*Chauvineau et al.,* 1993; *Scheeres,* 1994). An orbit with an opposite sense to the asteroid's orbital motion around the Sun (as it is for Petit Prince — Eugenia's spin is retrograde) is more stable against the effects of solar tides (*Hamilton and Burns,* 1991). Mechanisms for capture of such ejecta into quasi-stable orbits are reviewed by *Scheeres et al.* (2002).

The orbital period was determined to be ~4.7 d for the satellite of this FC-type asteroid and yields a density estimate of ~1.2 g cm^{-3} (*Merline et al.,* 1999c). This result fol-
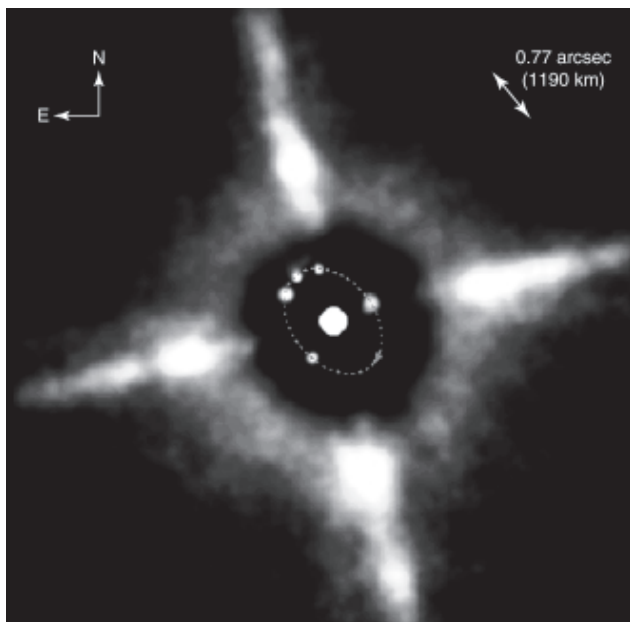
Fig. 5. This infrared image is a composite of five epochs of Eugenia's moon. The moon has a period of 4.7 d, with a nearly circular orbit of ~1190 km (0.77 arcsec). The orbit is tilted ~46° with respect to our line-of-sight. The normal two-fold degeneracy in pole position (i.e., true sense of the moon's orbit) was resolved by observing the system later, when positional differences between the two solutions became apparent. Eugenia is ~215 km in diameter and the moon's diameter is ~13 km. The large "cross" is a common artifact of diffraction from the secondary-mirror support structure. The images are deconvolved, and the brightness of Eugenia has been suppressed to enhance sharpness and clarity.
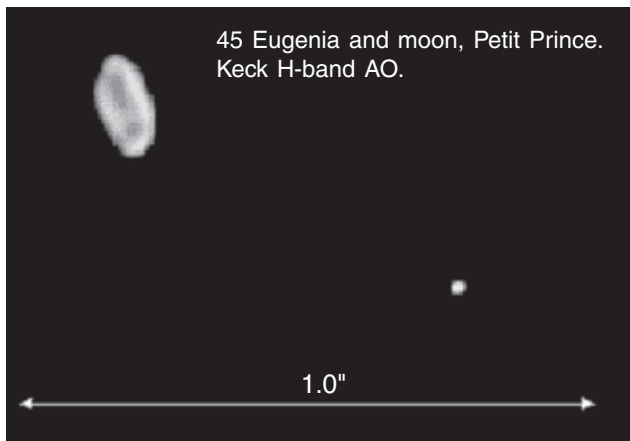
Fig. 6. This deconvolved Keck image in February 2000 shows Petit Prince (*Merline et al.,* 1999c) and a resolved image of the disk of Eugenia (after *Close et al.,* 2000). The pair is well separated enough to get accurate colors or spectra. The unusual elongation of Eugenia's shape was inferred previously from lightcurve amplitudes. Because the lack of detailed fidelity in flux preservation under deconvolution, the brightness variations across the disk are not real. The brightness of the satellite (which is not resolved) has been scaled to appear to have roughly the same "surface brightness" as the primary. The flux ratio of the two objects is about 285.

lowed soon after the surprising announcement that the density to C-type Mathilde was only 1.3 g cm⁻³, as determined by spacecraft flyby (*Veverka et al.,* 1999a). Such a density requires a significant amount of macroporosity to be consistent with the expected meteorite analog for these objects, namely carbonaceous chondrites (*Britt and Consolmagno,* 2000). Therefore, it is possible that these asteroids are loosely packed rubble piles.

2.2.3. (90) Antiope and (617) Patroclus. The first true double asteroid, (90) Antiope, was discovered in August 2000 by *Merline et al.* (2000a). This main-belt C-type was found to have two nearly equal-sized components of diameter ~85 km, rather than a single object of size 120 km as previously assumed. The orbital period of the pair was found to be ~16.5 h, consistent with the previously observed lightcurve period. Interestingly enough, a lightcurve by *Hansen et al.* (1997) shows a classic eclipsing-binary shape (although they did not make this interpretation), which would be expected to result from equal-sized components, with the orbit viewed edge-on. The derived density for the components of Antiope, assuming they are of the same size and density, is about 1.3 g cm⁻³, again similar to previous measurements of low-albedo asteroids. Figure 7 shows the components of Antiope as they orbit the common center of mass. Another double, (617) Patroclus, was discovered in September 2001 by *Merline et al.* (2001b). Again, it is a primitive P-type and is the first Trojan to be shown definitively to be binary. Few data were acquired, but it appears that this object also will show a low density.

2.2.4. (762) Pulcova, (87) Sylvia, and (22) Kalliope. Small satellites were also found around two more large, low-albedo asteroids: F-type (762) Pulcova (*Merline et al.,* 2000b) at CFHT and P-type (87) Sylvia (*Brown and Margot,* 2001) at Keck. Sylvia, a Cybele, is the first binary found in the outer main belt. In August/September 2001, a small companion to (22) Kalliope was discovered by *Margot and Brown* (2001) and *Merline et al.* (2001a). This is the first M-type asteroid known to have a companion and gives the hope of getting a reliable density estimate for these controversial objects, which have traditionally been thought to be metallic. Initial estimates put the density near ~2.3 g cm⁻³. This value is even lower, although not significantly, than the values previously derived for S-types (around 2.5 g cm⁻³). If so, it clearly indicates that at least Kalliope is not of a

Fig. 7. Double asteroid (90) Antiope as it rotates with a 16.5-h period, soon after its discovery at Keck in August 2000 (*Merline et al.,* 2000a,b). Once thought to be an object ~125 km across, the C-type asteroid Antiope actually has two components, each ~85 km in diameter. The separation is ~170 km.

solid metallic composition. It would also be difficult to imagine an extremely porous rubble pile of metallic composition, because it would imply a macroporosity of more than about 60%. We may be faced with the difficult task of explaining how bodies with metallic spectra and radar reflectivities have rocklike densities.

2.2.5. (3749) Balam. Among the main-belt binaries, this object stands out as an oddity. Discovered at Gemini Observatory in 2002 (*Merline et al., 2002*), this binary is the most loosely bound system known, even more so than the TNO binaries. The secondary appears to orbit at least 100 (primary) radii from the primary, which itself is rather small (about 7 km in diameter). This is probably the first system known that was formed by "disruptive capture," discussed in section 3.3. Early models of *Durda* (1996) and *Doressoundiram et al.* (1997), as well as the more sophisticated models currently being performed by Durda et al., indicate that such systems (small primaries, with a widely separated secondary) are commonly formed in catastrophic collisions and that a large number of should be found in the main belt.

2.2.6. Systematics. While there appears to be a rash of newly discovered binaries, it turns out that the prevalence of (large) main-belt moons is likely to be low, probably ~2% (*Merline et al., 2001d*). The largest survey to date, by Merline et al., has sampled more than 300 main-belt asteroids, with five examples of relatively large satellites (few

tens of kilometers in diameter). The overall frequency, including small, close-in moons such as Dactyl (currently unobservable from Earth), will undoubtedly rise, but it is unknown by how much. Very small satellites will have a limited lifetime against collisions, although it is possible they may reaccrete. The single known binary among the Trojans, from a sample of about six, hints that the binary frequency may be higher in that population, although it is noted that the collision speeds are comparable to the main belt and the collision frequencies are only higher by about a factor of 2 (*Davis et al., 2002*).

For those satellites that are found, it would be useful to establish any systematics that may provide clues as to the origin mechanism for the moons. For example, it has been suggested that either slow (from tidal spindown due to a satellite) or fast (from a glancing collision, which might form satellites) rotation might be correlated with the presence of satellites. Family members have been suggested as likely candidates for satellites, because coorbiting pairs may have been created in the family-forming event. The likelihood of moons may even be linked to the taxonomic type or shape of the asteroid.

Most of the observed binaries in the main belt, outer belt, or Trojan region are of primitive type (C, F, P). Are satellites truly more prevalent around these objects, or is there some observational selection effect? Clearly, those asteroids highest in priority for observation are the apparently

TABLE 1.   Binary asteroids discovered by adaptive optics or direct imaging techniques.

Object	Type	Taxonomic Classification (Tholen)	Family	Asteroid a (AU)	Primary Rotation Period (h)	Primary Diameter (km)	Discovery Date	Method
(243) Ida	MB	S	Koronis	2.86	4.63	31	Aug. 29, 1993	SC
(45) Eugenia	MB	FC	Eugenia	2.72	5.70	215	Nov. 1, 1998	AO
(762) Pulcova	MB	F		3.16	5.84	137	Feb. 22, 2000	AO
(90) Antiope	MB	C	Themis	3.16	16.50*	85 + 85	Aug. 10, 2000	AO
(87) Sylvia	OB	P		3.49	5.18	261	Feb. 18, 2001	AO
(107) Camilla	OB	C		3.48	4.84	223	Mar. 1, 2001	HST
(22) Kalliope	MB	M		2.91	4.15	181	Aug. 29, 2001	AO
(3749) Balam	MB	S	Flora	2.24		7	Feb. 8, 2002	AO
(617) Patroclus	L5-TROJ	P		5.23		95 + 105	Sep. 22, 2001	AO
1998 WW$_{31}$	TNO			44.95		150[†]	Dec. 22, 2000	DI
2001 QT$_{297}$	TNO			44.80		580[‡]	Oct. 11, 2001	DI
2001 QW$_{322}$	TNO			44.22		200[§]	Aug. 24, 2001	DI
1999 TC$_{36}$	TNO			39.53		740[‡]	Dec. 8, 2001	HST
1998 SM$_{165}$	TNO			47.82	7.98	450[‡]	Dec. 22, 2001	HST
1997 CQ$_{29}$	TNO			45.34		300[‡]	Nov. 17, 2001	HST
2000 CF$_{105}$	TNO			44.20		170[‡]	Jan. 12, 2002	HST

*Assuming synchronous rotation.
[†]Assuming, for both components, albedo ~5.4% and density ~1 g cm^{-3} (*Veillet et al., 2002*).
[‡]Values provided by A. W. Harris (personal communication, 2002), assuming albedo 4%.
[§]Assuming albedo 4% (*Kavelaars et al., 2001*).

MB = main belt; OB = outer belt; TROJ = Jupiter Trojan; TNO = transneptunian object; SC = spacecraft encounter; AO = adaptive optics; HST = HST direct imaging; DI = direct groundbased imaging.

TABLE 2.   Properties of secondaries and derived properties of primaries.

Object	Orbit a (km)	Orbit Period (d)	Orbit Size (a/R_p)	Orbit Sense	Moon Diameter (km)	Size Ratio (D_P/D_s)	Primary Mass ($\times 10^{16}$ kg)	Primary Density (g cm^{-3})	Mass Ratio (M/m)
(243) Ida	108	1.54	7.0	Prograde	1.4	22	4.2	2.6 ± 0.5	11,000
(45) Eugenia	1190	4.69	11.1	Prograde	13	17	610	1.2 ± 0.4	4900
(762) Pulcova	810	4.0	11.6		20	7	260	1.8 ± 0.8	340
(90) Antiope	170	0.69	4.0		85	1.0	41	1.3 ± 0.4	1.0
(87) Sylvia	1370	3.66	10.5		13	20	1500	1.6 ± 0.3	7900
(107) Camilla	~1000		~9		9	25			18,000
(22) Kalliope	1060	3.60	11.7	Prograde	19	10	730	2.3 ± 0.4	870
(3749) Balam	~350	~100	~100		1.5	4.6			95
(617) Patroclus	610	3.41	11.6		95	1.1	87	1.3 ± 0.5	1.3
1998 WW$_{31}$	22,300	574	300*		120*	1.2	170		1.7
2001 QT$_{297}$	~20,000		69†			1.4			2.6
2001 QW$_{322}$	~130,000	~1500§	1300‡		200*	1.0			1.0
1999 TC$_{36}$	~8000		22†			2.8			21
1998 SM$_{165}$	~6000		27†			2.4			14
1997 CQ$_{29}$	~5200		35†			~1?			~1?
2000 CF$_{105}$	~23,000		270†			1.6			3.9

*Assuming, for both components, albedo ~5.4% and density ~1 g cm^{-3} (*Veillet et al.,* 2002).

†Values provided by A. W. Harris (personal communication, 2002), assuming albedo 4%.

‡Assuming albedo 4% (*Kavelaars et al.,* 2001).

§This period is reasonable, despite the large observed separation, because of a high eccentricity (A. W. Harris, personal communication, 2002).

brighter objects. Among the objects in Merline et al.'s target lists, the S-like and C-like asteroids are about equal in number. (This may mean that the frequency of binaries is more like 4% among the primitive asteroids.) But this is not where the bias ends. To be of equal brightness, a C-like asteroid must be much larger than an S-like, and therefore will have a larger Hill sphere. As such, one can image deeper into the gravitational well of a C-like object than an S-like object of the same apparent brightness, on average. Given that most of the observed companions reside within about 12 primary radii, the companions of C-like objects will be more easily found. Nonetheless, if the frequency of companions were also 4% for the S-like asteroids, some should still have been found. This raises the question as to whether it is more difficult to make satellites around S-types, which may be predominantly fractured-in-place chards, rather than rubble piles (*Britt and Consolmagno,* 2001). If this is true, and because many of the outer-belt and Trojan asteroids are of primitive type, we may ultimately find a higher binary frequency among those populations.

Tables 1 and 2 summarize the properties of known binary systems discovered using adaptive-optics or direct-imaging techniques.

## 2.3.   Discovery by Direct Groundbased Imaging

Despite the difficulty of directly resolving a binary asteroid system from the ground without the assistance of adaptive optics, detections have recently been achieved. By direct imaging with CCDs on large telescopes under exceptional conditions, it has been possible to resolve TNO binaries. *Toth* (1999) discusses some of the issues regarding detectability of these objects. The first of these, 1998 WW$_{31}$, was discovered by *Veillet et al.* (2001) in December 2000 at CFHT. Followup observations of 1998 WW$_{31}$ from ground-based telescopes and HST, as well as archival searches of previous datasets, indicate that the system has a size ratio of about 1.2, with an eccentric (~0.8) orbit, a semimajor axis near 22,000 km, and a period of ~570 d (*Veillet et al.,* 2002).

Soon afterward, two more TNO binaries were detected in the same way: 2001 QT$_{297}$ (*Eliot et al.,* 2001), showing a separation of 0.6 arcsec at time of discovery and a size ratio of about 1.7; and 2001 QW$_{322}$ (*Kavelaars et al.,* 2001) with a size ratio of ~1.0 and a wide separation of 4 arcsec when discovered. Four additional TNO systems were subsequently discovered using HST (discussed in section 2.6). All of these systems, except one, are classical Kuiper Belt objects, residing at ~45 AU. One system, 1999 TC$_{36}$, is a Plutino at ~40 AU.

For these objects, AO cannot be used directly because they are too faint, so direct imaging, either from the ground or in ongoing campaigns on the HST, is likely to be the most attractive approach. Because they move slowly past field stars, it is possible to use AO to image these objects during appulses with brighter stars. This technique may improve the overall sensitivity to fainter companions.

The size of the Hill sphere of an object is directly proportional to its distance r from the Sun, but the angular size
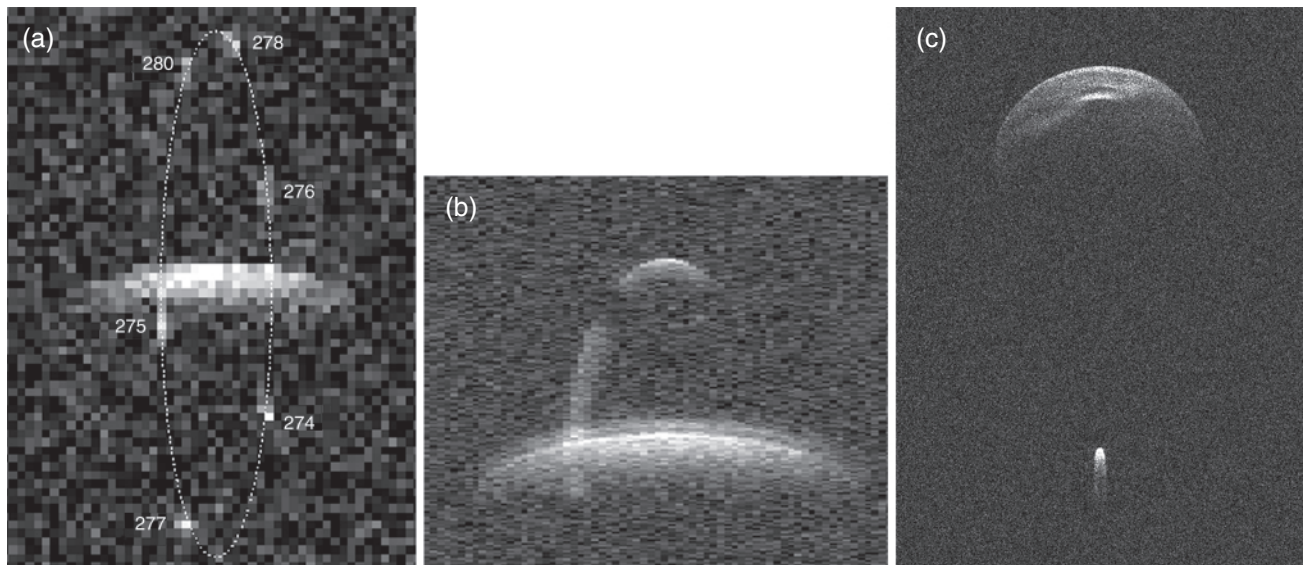
Fig. 8. **(a)** Arecibo delay-Doppler images of binary asteroid 2000 DP$_{107}$ (*Margot et al.,* 2002b) obtained on 2000 DOY 274-280. A dashed line shows the approximate trajectory of the companion on consecutive days. **(b)** Goldstone radar echoes of 1999 KW$_4$ (S. Ostro et al., personal communication, 2001) accumulated over several hours during its May 2001 close approach to Earth. **(c)** Radar image of 1999 KW$_4$ obtained at Arecibo on May 27, 2001, with 7.5-m range resolution. Range from the observer increases down and Doppler frequency increases to the right. Dimensions in the cross-range dimension are affected by the primary and secondary spin rates.

of a satellite orbit, as seen from Earth is inversely proportional to the distance from the observer, Δ, which is approximately r. So if satellites reside at the same fraction of their Hill sphere from the primary, there should be no advantage of direct imaging in observing outer solar system objects compared with similar-sized objects in the main belt. Apparently, the main reasons these systems are being found with direct imaging, while those in the main belt are not, is that the secondary to primary size ratios are high, making the secondary easier to detect, while at the same time the satellites are more loosely bound. Additionally, the TNO primaries are rather large, further assisting detection because of the correspondingly larger Hill sphere. Possibly, similar systems are rare in the main belt, and the TNO binaries are formed by a different process.

2.4. Radar Discovery and Characterization of Binary Near-Earth Asteroids

The radar instruments at Goldstone and Arecibo recently provided the first confirmed discoveries of binary asteroids in the near-Earth population (*Margot et al.,* 2002a,b). In the two-year period preceding this writing, six near-Earth objects have been unambiguously identified as binary systems: 2000 DP$_{107}$ (*Ostro et al.,* 2000b; *Margot et al.,* 2000); 2000 UG$_{11}$ (*Nolan et al.,* 2000); 1999 KW$_4$ (*Benner et al.,* 2001a); 1998 ST$_{27}$ (*Benner et al.,* 2001b); 2002 BM$_{26}$ (*Nolan et al.,* 2002a); and 2002 KK$_8$ (*Nolan et al.,* 2002b). Previous attempts to detect asteroid satellites with radar date back to the search for a synchronous moon around Pallas (*Showalter et al.,* 1982). S. Ostro (personal communication, 2001) recalls that concrete anticipation for the radar dis-

covery of binary systems arose with the imaging and shape modeling of the strongly bifurcated NEA (4769) Castalia (*Ostro et al.,* 1990; *Hudson and Ostro,* 1994). *Ostro et al.* (2002) provide a thorough description of radar observations of asteroids.

In continuous-wave (CW) datasets, in which echoes resulting from a monochromatic transmission are spectrally analyzed, the diagnostic signature is that of a narrowband spike superposed on a broadband component. The wide-bandwidth echo is distinctive of a rapidly rotating primary object, i.e., with spin periods of order a few hours. The narrowband feature, which does not move at the rate associated with the rotation of the primary, represents power scattered from a smaller and/or slowly spinning secondary. As time goes by, the narrowband echo oscillates between negative and positive frequencies, representing the variations in Doppler shift of a moon revolving about the system's center of mass (COM). The timescale associated with this motion in the small sample of objects studied so far is on the order of a day.

In delay-Doppler images, in which echo power is discriminated as a function of range from the observer and line-of-sight velocity, the signatures of two distinct components are easily observed. Both the primary and secondary are typically resolved in range and Doppler, and their evolution in delay-Doppler space is consistent with the behavior of an orbiting binary pair. Example datasets are shown in Fig. 8.

The observables that can be measured from radar images are (1) visible range extents, which constrain the sizes of each component; (2) Doppler bandwidths, which constrain the spin periods of both the primary and secondary;

TABLE 3.   Binary asteroids detected by radar.

Object	a (m)	e	P_{orb} (d)	$(M_1 + M_2)$ $(10^9$ kg)	R_p (m)	R_s (m)	a/R_p	ρ (g cm^{-3})
2000 DP$_{107}$	2622 ± 54	0.010 ± 0.005	1.755 ± 0.002	460 ± 50	400 ± 80	150	6.6	1.7 ± 1.1
2000 UG$_{11}$	337 ± 13	0.09 ± 0.04	0.770 ± 0.003	5.1 ± 0.5	115 ± 30	50	2.9	0.8 ± 0.6
1999 KW$_4$	2566 ± 24	≤0.03	0.758 ± 0.001	2330 ± 230	600 ± 120	<200	4.3	2.6 ± 1.6
1998 ST$_{27}$	4000–5000				250–300	<50	13–20	
2002 BM$_{26}$			<3		300	50		
2002 KK$_8$					500	100		

Orbital parameters for radar-observed binary NEAs, including semimajor axis in meters, eccentricity, orbital period in days, and inferred total mass. Size and density estimates of the primary are also listed.

(3) range and Doppler separations as a function of time, which characterize the system's total mass and orbital parameters; and (4) reflex motion of the primary about the COM, which constrains the mass ratio of the system. Although the location of the COM is initially uncertain, the process of ephemeris refinement quickly leads to a very precise knowledge of its position in each image frame.

The bulk of the data analysis so far has concentrated on using the range and Doppler separations to fit for the system's total mass and orbital parameters. The model assumes that the orbital motion of the secondary takes place in a plane with an orientation that remains fixed in inertial space during the time of the observations. Such mass estimates, coupled with a detailed knowledge of the component volumes from shape-modeling techniques (*Hudson,* 1993), can lead to precise asteroid density measurements. The density values presented here rely on size estimates from visual inspection of the raw radar images and on the verifiable assumption that most of the system's mass belongs to the primary object.

The current best-fit orbital parameters along with the formal errors of the fit are presented in Table 3. All solutions have χ-squared values of ≃1. The best-fit mass and density estimates are also shown.

The binary systems observed with radar so far share similar characteristics. The primary components all appear roughly spheroidal and have spin periods near the breakup limit. The secondaries have diameters on the order of one-third the diameter of the primary. All radar-observed NEA binaries have satellites orbiting at a distance of a few primary radii. Their orbital periods are on the order of a day. Because the spin periods of the primary are typically a few hours, the systems observed to date cannot be mutually synchronous. The spin periods of the secondaries are indicative of spin-lock configurations, which is consistent with calculations of tidal despinning timescales (*Margot et al.,* 2002b).

The proportion of binary objects among radar-observed NEAs larger than 200 m is ~16% (*Margot et al.,* 2002b). This large proportion requires the formation of binaries to be frequent compared to the ~10-m.y. dynamical lifetime of NEAs. Radar observations show that binary NEAs have spheroidal primaries spinning near the breakup point for strengthless bodies, suggesting that the binaries formed by spinup and fission, probably as a result of tidal disruption during close planetary encounters (section 3.1).

The ability to determine the orientation of the orbital plane using radar depends critically on the plane-of-sky coverage. For 2000 DP$_{107}$, which had a sky motion of ~40° during radar observations, the orientation of the orbital plane can be constrained to within a 28° cone. In the case of 2000 UG$_{11}$ and 1999 KW$_4$, with ~60° and ~110° of sky motion respectively, pole solutions are expected to be better constrained. For 2000 DP$_{107}$ and 1999 KW$_4$, one cannot reject the hypothesis that the orbit is circular, but for 2000 UG$_{11}$ that same hypothesis can be rejected at better than the 1% level.

Reflex motion of the primary is clearly observed in the radar datasets, providing the exciting prospect of measuring the densities of NEA satellites. Improved orbital fits will incorporate the residual motion of the primary with respect to the COM and will include the mass ratio of the system as an additional parameter.

Additional improvements are expected from shape reconstruction techniques (*Hudson,* 1993), in which a series of delay-Doppler images are inverted in a least-squares sense to provide a shape model. Given images with sufficient signal-to-noise ratio and orientation coverage, it is possible to infer shape and spin information for the satellites and to derive solid conclusions regarding spin-orbit resonances. Apart from possibly yielding clues on formation mechanisms, shape models will significantly decrease the uncertainties associated with size/volume estimates, and this will result in considerably lower error bars on the initial density measurements presented here.

The techniques for extracting information about binary systems from the radar data are still very much under active development. At this early stage, it appears that one weakness of the radar method lies in its inability to constrain unambiguously the orientation of the orbital plane, particularly when sky motion is limited. This is an intrinsic limitation of range and line-of-sight velocity measurements obtained without angular leverage. Observations over a range of aspect angles can overcome this ambiguity. The detection of occultations in the radar data or of occultations or eclipses from lightcurve observations can also place tight constraints on the inclination of the orbit. In general, a combination of radar and lightcurve observations will yield

the best orbital determinations. The radar data may in turn help the interpretation of lightcurve profiles by distinguishing occultations from eclipses and primary from secondary events. Interesting synergies are therefore expected from the combination of the radar and lightcurve techniques. Because radar shadows are cast in much the same way as their optical counterparts, radar occultations of binary systems will be observed sooner or later, in which case the orientation of the orbital plane would be very tightly constrained.

Radar observations of binary asteroids constitute an emerging field that holds great promise for the future. The information that can be gathered from radar datasets includes determination of bulk properties (e.g., density, rigidity), and of orbital/spin characteristics, of both components. Combined with high-resolution imaging and shape models, these are providing powerful constraints on the formation mechanisms of binary NEAs. The characteristics of eccentricity and spin damping provide insightful clues about the internal structure of asteroids.

2.5. Binary Asteroids Detected by Lightcurves

Serious attempts to reveal the binary nature of some asteroids from their lightcurve features date back to the 1970s (cf. *Cellino et al.,* 1985). A review of the advantages and disadvantages of various methods of extracting such information from asteroid lightcurves is given by *Weidenschilling et al.* (1989). Recent advances in methods for interpretation of lightcurves can be found in *Kaasalainen et al.* (2002). While most techniques have not led to a successful detection of a binary asteroid, one of them, mentioned in the end of section IV.B of *Weidenschilling et al.* (1989), has been recently successful — the detection of nonsynchronous satellites.

Pravec (1995) analyzes a two-period lightcurve of the NEA 1994 AW_1, measured by *Mottola et al.* (1995) and *Pravec et al.* (1995), and interprets the complex lightcurve as being due to occultation/eclipse events in a binary asteroid system combined with a fast rotation of the primary. The results were published also in *Pravec and Hahn* (1997), who present the binary hypothesis as the likely explanation of the 1994 AW_1 lightcurve but also consider the possibility that it might be an asteroid in a complex rotation state. In light of more recent results (see below), the binary status of 1994 AW_1 is quite likely and we consider it to be the first binary asteroid detected by the lightcurve technique. See Table 4 for estimated parameters of this binary system.

The second binary asteroid found from lightcurve observations is 1991 VH (*Pravec et al.,* 1998a). Extensive photometric observations show that the asteroid's lightcurve is doubly periodic and that its long-period component shows occultation-like features; Pravec et al. interpret the data as evidence that 1991 VH is an asynchronous binary system,

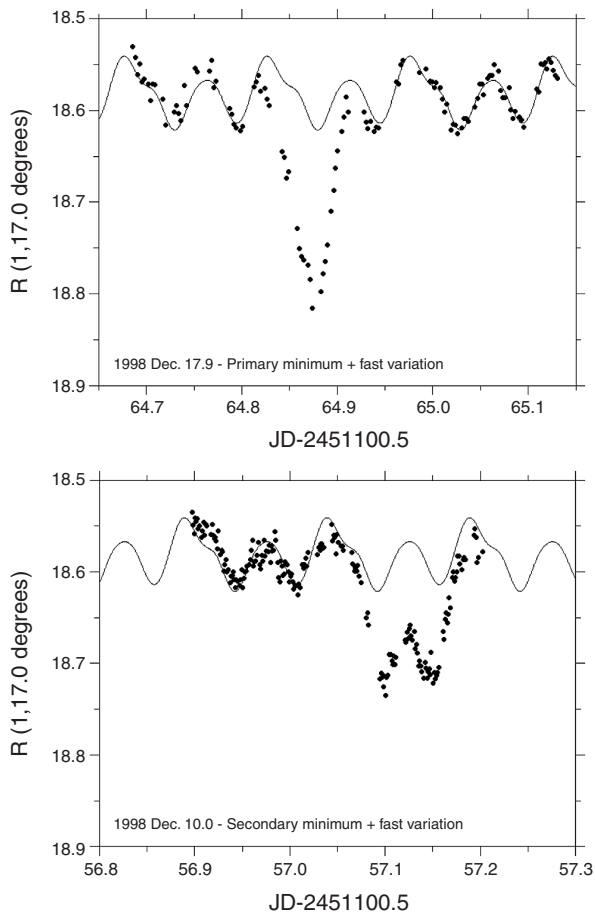TABLE 4. Estimated parameters of binary NEAs, detected by lightcurve.

Object	D_p (km)	D_s/D_p	a/R_p	e	P_{orb} (h)	P_{rot} (h)	A_{rot} (mag)	Taxonomic Class	Orbital Type	References
1994 AW_1	0.9	0.53	4.6	<0.05	22.40	2.5193	0.16		PHA	[1]
1991 VH	1.2	0.40	5.4	0.07	32.69	2.6238	0.11		PHA	[2]
(3671)	0.9	>0.28	5.2		27.72	2.7053	0.16	EM	PHA	[3,12,13]
1996 FG_3	1.4	0.31	3.4	0.05	16.14	3.5942	0.09	C	PHA, VC	[4,5]
(5407)	4.0	≥0.30	(3.4)	(<0.05)	(13.52)	2.5488	0.13	(S)	MC	[4]
1998 PG	0.9	≥0.30	(3.4)		(14.01)	2.5162	0.13	S	Amor	[4]
1999 HF_1	3.5	0.24	4.0		14.02	2.3191	0.13	EMP	Aten, VC	[6]
2000 DP_{107}	0.8	0.38	6.6	0.01	42.2	2.7755	0.22	C	PHA	[7,8,14]
2000 UG_{11}	0.23	≥0.6	3.6	0.12	18.4	(4.44)	0.10	QR	PHA	[13,14]
1999 KW_4	1.2	≥0.3	4.2	≤0.03	17.45	2.765	0.13	Q	PHA, VC	[9,10,13,14]
2001 SL_9	1.0	0.31	3.6		16.40	2.4003	0.09		Apollo	[15]

References: [1] *Pravec and Hahn* (1997); [2] *Pravec et al.* (1998a); [3] *Mottola et al.* (1997); [4] *Pravec et al.* (2000a); [5] *Mottola and Lahulla* (2000); [6] *Pravec et al.* (2002a); [7] *Margot et al.* (2002b); [8] *Pravec et al.* (2000b); [9] *Benner et al.* (2001a); [10] *Pravec and Šarounová* (2001); [11] *Harris and Davies* (1999); [12] P. Pravec et al. (unpublished data, 1997); [13] *Margot et al.* (2002a); [14] P. Pravec et al. (personal communication, 2002); [15] *Pravec et al.* (2001).

The diameter of the primary D_p was estimated from the effective diameter 1.0 km given by *Harris and Davies* (1999) for (3671), and from measured absolute magnitudes assuming the geometric albedo p = 0.06 for 1996 FG_3, and 2000 DP_{107}, and p = 0.16 for the other objects; it was corrected for D_s/D_p = 0.4 in cases where only a lower limit on the secondary-to-primary diameter ratio is available. a is the semimajor axis of the mutual orbit, e is its eccentricity, P_{orb} is the orbital period. P_{rot} is the rotation period of the primary, A_{rot} is its amplitude corrected for contribution of the light from the secondary. The values in brackets are derived using the assumptions discussed in *Pravec et al.* (2000a). PHA stands for potentially hazardous asteroid, which is an object approaching closer than 0.05 AU to the Earth's orbit, VC stands for Venus-crosser, MC stands for Mars-crosser. This table has been updated from *Pravec et al.* (2000a). For uncertainties and assumptions made with the estimates, see the original publications. Note that some of these objects are in common with NEAs observed by radar, in Table 3. An updated, combined radar/lightcurve NEA table is maintained at http://www.asu.cas.cz/~asteroid/binneas.htm.

similar to 1994 AW$_1$. The same or similar observational and analysis techniques have been used to reveal the binary nature of several other objects, shown in Table 4. The general technique has been validated by the radar detection of the binary status of 2000 DP$_{107}$, for which *Pravec et al.* (2000b) and P. Pravec et al. (personal communication, 2002) observe a two-period lightcurve of the same kind as in the previous cases and estimate parameters of the binary system that are in agreement with results from the radar observations.

This lightcurve technique for detecting binaries has been described in the above-mentioned papers as well as in more recent works by *Pravec et al.* (2000a) and *Mottola and Lahulla* (2000). Briefly, it is based on detecting brightness attenuations caused by mutual occultations or eclipses between components of the binary system superposed on the short-period rotational lightcurve of the primary. An example is shown in Fig. 9. The principles of the technique introduce several selection effects. The technique can reveal the existence of large satellites around asynchronously rotat-

ing primaries only under favorable geometric conditions. Another bias is that detection of close binary systems is favored, because observations and their interpretation are easier for systems with shorter orbital periods. Satellites smaller than ~20% of the primary diameter are difficult or impossible to detect unambiguously from lightcurve observations because they produce only small brightness attenuations during occultations or eclipses, less than ~0.04 mag. This may be difficult to separate from other effects, like an evolution of the primary's rotational lightcurve in changing observational geometric conditions. The asynchronous rotation of the primary allows one to resolve the occultation/eclipse events, which occur with a period different from the rotation period of the primary, and therefore one may rule out their possible connection with any peculiar shape feature of the primary. Occultations or eclipses can be observed only when the Earth or Sun, respectively, lie close enough to the mutual orbital plane of the binary system. These selection effects mean that there may be a bias toward binary systems with certain favorable parameters in the sample of known or suspected binary asteroids presented in Table 4. Nevertheless, at least some of the similarities of the characteristics of the binary asteroids cannot be explained by selection effects alone and must be real.

The similarities of the 13 NEA binary asteroids, known or suspected from lightcurve or radar observations, are:

1. They are small objects with primary diameters 0.7–4.0 km. The lower limit may be due to a bias against detection of small binary systems, because fainter asteroids are normally more difficult to observe. There may exist an upper limit but it is difficult to estimate from the small sample.

2. They all are inner planet-crossers. Most of them approach the orbits of Earth and Venus. This feature may be due, at least partly, to a selection effect, as kilometer-sized asteroids are much easier to observe in near-Earth space than in the main belt. Another possible selection effect is that more observations are being made, in general, of near-Earth objects.

3. All the primaries are fast rotators (periods 2.3–3.6 h), not far below the critical stability spin rate, with low amplitudes (0.1–0.2 mag), suggesting nearly spheroidal shapes (see *Pravec et al.,* 2002b).

4. The secondary-to-primary diameter ratios are almost all in the range of 0.2–0.6. While the lower limit may be just a result of the selection effect mentioned above, it appears that binaries with nearly equal-sized components are rare among kilometer-sized NEAs. The probability that there are twelve objects with the diameter ratios in the range of 0.2–0.6 and one in 0.6–1.0, for a uniform distribution of diameter ratios, is less than 0.2%.

5. Semimajor axes estimates are in the range 3.4–6.6 primary radii. While the upper limit may be due to the selection effect mentioned above, the lower limit (corresponding to orbital periods ~14 h) may be real, and it suggests that very close binary systems are not present (perhaps due to their instabilities).

6. Eccentricities are poorly constrained but appear to be low (less than 0.1).

Fig. 9. Observed lightcurves of 1996 FG$_3$ show the fast-variation, small-amplitude component, caused by the rotation of the primary, with superposed sudden sharp attenuations caused by the eclipse/occultation of the primary by the secondary. The top panel shows the primary minimum, while the bottom panel shows the secondary minimum. The primary rotation component can be seen also during the attenuations. (From *Pravec et al.,* 2000a.)

Pravec et al. (1999) accounted for the bias due to the selection effect related to the geometric observing conditions and estimated, on the basis of the first three known binary NEAs, that the fraction of binaries among NEAs is ≈17% with an uncertainty factor of 2. This is consistent with the estimates from radar data that ~16% of NEAs are binary (*Margot et al.,* 2002b), and the estimates (about 15%) of *Bottke and Melosh* (1996a,b) from models of binary production by tidal disruption (see section 3.1). Based on these studies, we adopt 16% as our working estimate of the NEA binary fraction. We note that ~30% of kilometer-sized asteroids are fast rotators with periods <4 h and that binary NEAs have fast-rotating primaries. Therefore, it may be that roughly half of the fast-rotating NEAs are binary (*Pravec and Harris,* 2000) and that binary asteroids are common among fast-rotating objects on Earth-approaching orbits.

2.6. Hubble Space Telescope (HST) Companion Searches

One of the major projects that *Zellner et al.* (1989) expected to be addressed by HST was the search for asteroid companions. The absence of atmospheric effects on HST images allows diffraction-limited operation over a very large field of view. The spherical aberration of the primary mirror did not stop the execution of an early attempt to survey the asteroid belt (program 4521) as well as an "amateur" program that targeted asteroids thought to have companions, primarily from occultation observations (program 4764). No companions were found but careful restoration of the data was necessary to minimize the effects of the aberration. While aberration did not limit the spatial resolution of the images (the middle two-thirds of the primary was ground correctly), the additional "skirt" of scattered light did limit the dynamic range over which a companion could be detected.

Storrs et al. (1999a) published the data from these two programs. Their reconstruction of the HST images allowed upper limits to be put on the presence of companions to asteroids (9) Metis, (18) Melpomene, (19) Fortuna, (109) Felicitas, (146) Lucina, (216) Kleopatra, (434) Hungaria, (532) Herculina, (624) Hektor, and (674) Rachele. No companions were found to a brightness limit that varied with distance from the primary, as shown in Fig. 10. Barring the companion being in conjunction at the time of observation, Storrs et al. rule out companion objects (suggested by early occultation observations) to asteroids (9) Metis, (18) Melpomene, and (532) Herculina (the brightness and separation of suggested companions are designated by the numbers in Fig. 10).

Program 6559 (*Storrs et al.,* 1998, 1999b) detected no companions to the eight asteroids imaged by HST with the corrected Wide Field Planetary Camera 2 (WFPC2) instrument. Further HST imaging observations are currently under way in program 8583, which is a "snapshot" program designed to fill in gaps in the spacecraft's calendar of observations. The program targets 50 large, main-belt asteroids (many of them twice) with the WFPC2 in a manner simi-
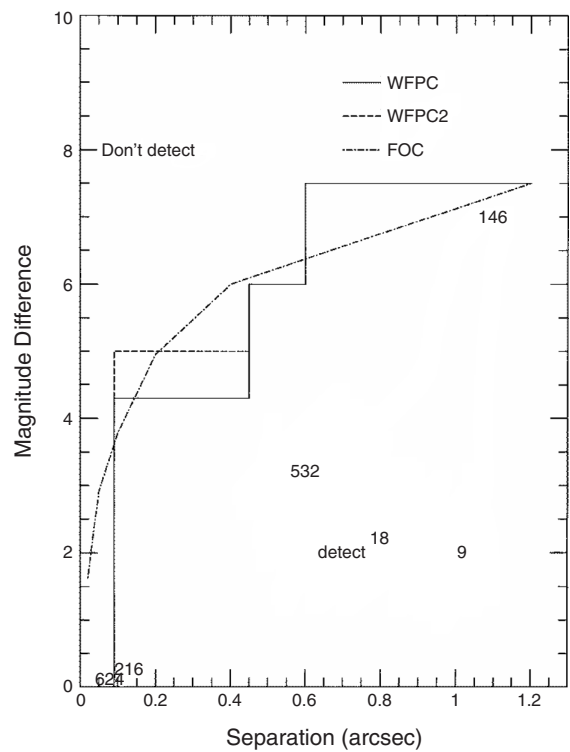
Fig. 10. Brightness difference (in magnitudes) between a primary asteroid and a possible companion as a function of projected distance from the primary asteroid, for well-exposed HST images (after *Storrs et al.,* 1999a). The region below the curves is where companions could be detected. Also shown are the locations of putative binaries (given by asteroid number) previously suspected from occultation or other data.

lar to that used to map (4) Vesta by *Binzel et al.* (1997). This program resulted in the discovery of a companion to (107) Camilla (*Storrs et al.,* 2001a) and confirmed observations of companions to (87) Sylvia (*Storrs et al.,* 2001b) and (45) Eugenia. The companions to (45) Eugenia and (107) Camilla have the same color in the visible range as their primaries. *Storrs et al.* (2001b) report that the companion to (87) Sylvia appears significantly bluer than its primary. The observations of (6) Hebe in this program reveal no companions brighter than 7 mag fainter than the primary, or larger than 8 km in diameter.

Another program for observing main-belt asteroids, that of Zappalà and colleagues, used the HST Fine Guidance Sensor (FGS). The first results of this program confirmed that (216) Kleopatra is a contact binary (*Tanga et al.,* 2001). Two other programs are under way, both of them targeting TNOs; both began to detect binaries in early 2002. A large program by M. Brown has detected two TNO companions: 1999 TC$_{36}$ (*Trujillo and Brown,* 2002) and 1998 SM$_{165}$ (*Brown and Trujillo,* 2002). In a second program, two more binaries have been found: 1997 CQ$_{29}$ (*Noll et al.,* 2002a) and 2000 CF$_{105}$ (*Noll et al.,* 2002b). As in the case of the other known TNO binaries, these objects have a wide separation and relatively large secondaries.

The strengths and weaknesses of HST/WFPC2 observations of asteroids are discussed in *Dotto et al.* (2002). Briefly, WFPC2 observations allow diffraction-limited observation over a large field of view from the vacuum UV to beyond 1-μm wavelength. These high-resolution images can provide information on the shape and mineralogical variegation of the primary as well. Drawbacks include the robotic nature of HST scheduling (ephemerides good to better than 10 arcsec for over a year are necessary to find the asteroid), no sensitivity beyond 1 μm [but see *Dotto et al.* (2002) for a discussion of WF3, which will operate to 1.8 μm], and the difficulty in getting observing time on HST (no immediate follow up of detections). HST observations are complementary to groundbased AO observations because they cover a larger field of view per exposure at a shorter wavelength, but cannot cover the critical near-IR wavelength region.

2.7.   Role of Occultations

Described as a technique of searching for asteroid satellites by *Van Flandern et al.* (1979) in *Asteroids*, the method of using stellar occultations suffers from the inability to plan or repeat an experiment, at least reliably. *Reitsema* (1979) has called into question many of the early reports of satellites, indicating that the measurements are susceptible to spurious events. One-time reports of occultations can serve only to alert more rigorous search methods of a potential candidate. In addition, once an asteroid is known to have a moon, systematic networks of observers may be placed as to attempt to see an event from the moon during an occultation of the primary. These observations could greatly constrain our understanding of the sizes and positions of the satellites.

It is important to note, however, that archived occultation records (D. Dunham, personal communication, 2001) have shown that two short events have been recorded accompanying an occultation of Eugenia (diameter 215 km). One was in 1983 (chord equivalent ~9 km) and another in 1994 (chord equivalent ~20 km). Another short event, of chord size 18 km, was recorded in 1997 during an occultation of Sylvia (diameter 271 km). The satellite diameters predicted from AO observations are 13 km for Eugenia and 13 km for Sylvia. It is unlikely that such short chords would have resulted from asteroids of this large size. Therefore, it is possible that these occultations in fact did record satellite events.

3.   ORIGIN AND EVOLUTION OF BINARY ASTEROIDS

In *Asteroids II*, *Weidenschilling et al.* (1989) discussed the most promising mechanisms for formation of asteroid binaries. Most of the progress since that time has been observational, but theoretical efforts, especially numerical modeling, have also made advances. With the new examples of actual binary systems to study, there has recently been a renewed interest in theories of formation and in numerical modeling of binary origin. All of the formation mechanisms discussed by Weidenschilling et al. remain viable. Here we revisit these and add others.

3.1.   Near-Earth Asteroids: Tidal Encounters

As discussed in sections 2.4 and 2.5, a significant fraction (16%) of NEAs appear to be binary. This is much higher than their apparent abundance in the main belt (although detection is more difficult for the latter), but is consistent with the fraction of recognized doublet craters in impacts on Earth (*Weidenschilling et al.,* 1989). Apparently, some mechanism favors production of binaries among planet-crossers (unless it is possible to get small main-belt binaries to be ejected from the belt intact). A close planetary encounter can subject an asteroid to tidal stresses and torques that may produce a binary. The same process, however, can also disrupt existing binary systems. Because the lifetime of NEAs is relatively short (a few times 10^7 yr) and close encounters are more probable than planetary impacts, this formation/destruction is an equilibrium process. *Bottke and Melosh* (1996a,b) examine the effect of planetary encounters on contact binaries (two components) and conclude that ~15% of Earth-crossers evolve into coorbiting binaries. *Richardson et al.* (1998) and *Bottke et al.* (1999), model the tidal disruption of ellipsoidal rubble-pile asteroids (composed of many small, equal-sized particles) encountering Earth and find that rotational spin-up frequently cause them to undergo mass shedding. In many cases, some of the shed fragments go into orbit around the progenitor, producing binary asteroids. Most of these satellites, however, are much smaller than the primary. Also, the yield of binaries is low; disruption into a string of clumps, as for comet Shoemaker-Levy 9, is more probable than binary formation. The results of these studies suggest that tidal disruption can produce enough binaries to account for the observed population of doublet craters on the terrestrial planets, provided that small asteroids (less than a few kilometers in diameter) are not finely divided gravel piles, but "coarse" structures dominated by a few large chunks. This inference is also consistent with their observed maximum rotation rates (cf. *Paolicchi et al.,* 2002).

3.2.   Cratering Ejecta

A cratering event from a subcatastrophic impact on an asteroid produces ejecta with a range of velocities. It is therefore likely that some of the ejecta will have sufficient kinetic energy and angular momentum to go into orbit about the target body. Except in highly oblique impacts, the ejecta leave the crater with a more or less uniform azimuthal distribution as seen in the frame of the target's surface. If the target is rotating, the rotational velocity of the surface at the impact point is added to the ejecta velocity; therefore, more mass will attain orbital velocity in the prograde direction (we assume that the impact is not large enough to

make a significant change in the target's rotational state). The problem with this model is how to place the ejecta into stable orbits. If the target is a sphere with a purely radial gravity field, then the ejecta particles have elliptical orbits that would intersect the surface after one revolution. Collisions between fragments, as well as solar perturbations acting on particles with highly eccentric orbits, might prevent immediate reimpact, but these apparently inefficient mechanisms would have to act during the first orbit after the impact. However, many asteroids are significantly nonspherical (triaxial) in shape and usually rotate about their shortest axis. This means that ejecta particles experience a noncentral gravity field, which can significantly alter their orbital parameters on the timescale of a single orbit. Also, a particle launched from a point near the longer equatorial axis may encounter a shorter axis during its first few periapse passages, avoiding impact and prolonging its lifetime. Mutual collisions among fragments during the first few orbits can dampen their eccentricities, yielding orbits that no longer intersect the primary's surface. This material could then accrete into a small satellite. As pointed out by *Weidenschilling et al.* (1989), ejecta velocities must be within the limited range that allows material to go into orbit about the primary without escaping completely. Such orbits have specific angular momentum corresponding to circularized orbits within a distance of about 2 radii from the primary. Unless this distance is outside the synchronous point, any satellite that accreted in this manner would be subject to tidal decay and would eventually collide with the primary. The requirement that the synchronous distance lies within 2 radii implies a spin period of not more than ~6 h. Tidal torque would then cause the satellite to migrate outward; for small secondary/primary mass ratios, the primary's spin would not be slowed significantly. Thus, satellites formed by this mechanism would be small rubble piles in prograde orbits about rapidly rotating primaries. In addition to these criteria listed by Weidenschilling et al., we add the requirement that the primaries be significantly nonspherical.

In a preliminary numerical study to explore the viability of this mechanism for producing small satellites, *Durda and Geissler* (1996) examined the accretion of ejecta particles from three different 10-km-scale craters on Ida. In each case they followed the dynamical evolution of 1000 ejecta particles for 100 h after the cratering impact and searched for "collisions" between orbiting particles, treating each "collision" as an accretion event. That study found that temporary aggregates containing ~0.1% of the ejected debris mass did indeed form while in flight around the primary, but none of these aggregates occupied stable orbits and survived [although the temporary aggregates were primarily on prograde trajectories concentrated near the equatorial plane of Ida, as predicted by *Weidenschilling et al.* (1989)]. The failure of the model to yield small satellites via accretion of ejected cratering debris may not be evidence that this mechanism fails to work or is incredibly inefficient, but instead may be a result of the approximations inherent to the model (the Dactyl-forming impact may

also have been larger than modeled). Indeed, several processes that subsequently have been shown to play important roles in placing material into bound orbits (e.g., distortion of the primary's shape, vaporization of some fraction of material, impact angle) were not included in the modeling. Instead, the Durda and Geissler model, which has proved quite successful in explaining the distribution of ejecta on Ida's surface (*Geissler et al.,* 1996), simulated the ejection of crater debris from various locations on Ida by launching particles from a point at a 45° angle to the local surface. The particles were all launched at the same instant at the beginning of the simulations, with no momentum transfer to the asteroid. In reality, excavation flows encompass the entire center-to-rim extent of a crater, the timescale for crater excavation on a low-gravity object can approach a significant fraction of the asteroid rotation period, and translational and rotational momentum is imparted to the primary during the impact (e.g., *Asphaug et al.,* 1996; *Love and Ahrens,* 1997). Thus, a combination of shape/distortion effects and translational/rotational motion during the excavation phase may play an important role in allowing particles to remain in temporary orbit.

This mechanism would operate in the environment of high-velocity impacts in the present main belt. Impacts are also capable of destroying small satellites, which would have shorter lifetimes against disruption than their primaries (although they might reaccrete after such events if the fragments remain in orbit). Thus, we expect the population of such binaries to be in equilibrium between formation and destruction by impacts.

Of the main-belt asteroids known to be binaries, six of eight (22, 45, 87, 107, 243, and 762) have satellites much smaller than their primaries. Assuming equal albedos and densities for both components, the mass ratio is typically ~10^{-3}. Significantly, all the primaries are rapid rotators; the longest period is 5.84 h for (762) (*Davis,* 2001). Also, they have rather large amplitude lightcurves, with maximum observed amplitudes of at least 0.25 mag. These properties are consistent with the formation of their satellites from impact ejecta. If the direction of an orbit relative to the rotation of the primary is found to be prograde, this would be a strong indication of their origin by this mechanism. The sense of the orbit is known for three of these main-belt binaries. The moons of (243) Ida (*Belton et al.,* 1995, 1996), (45) Eugenia (*Merline et al.,* 1999b,c), and (22) Kalliope orbit in a prograde sense.

3.3. Disruptive Capture

Many asteroids belong to dynamical families that reveal them to be fragments of larger parent bodies that were disrupted by catastrophic collisions. In such a disruptive event, fragments may end up in orbit about each other, as suggested by *Hartmann* (1979). *Weidenschilling et al.* (1989) point out that in a radial-velocity field of fragments escaping from a disrupted primary, geometrical constraints imposed by the finite sizes of fragments would tend to ensure that
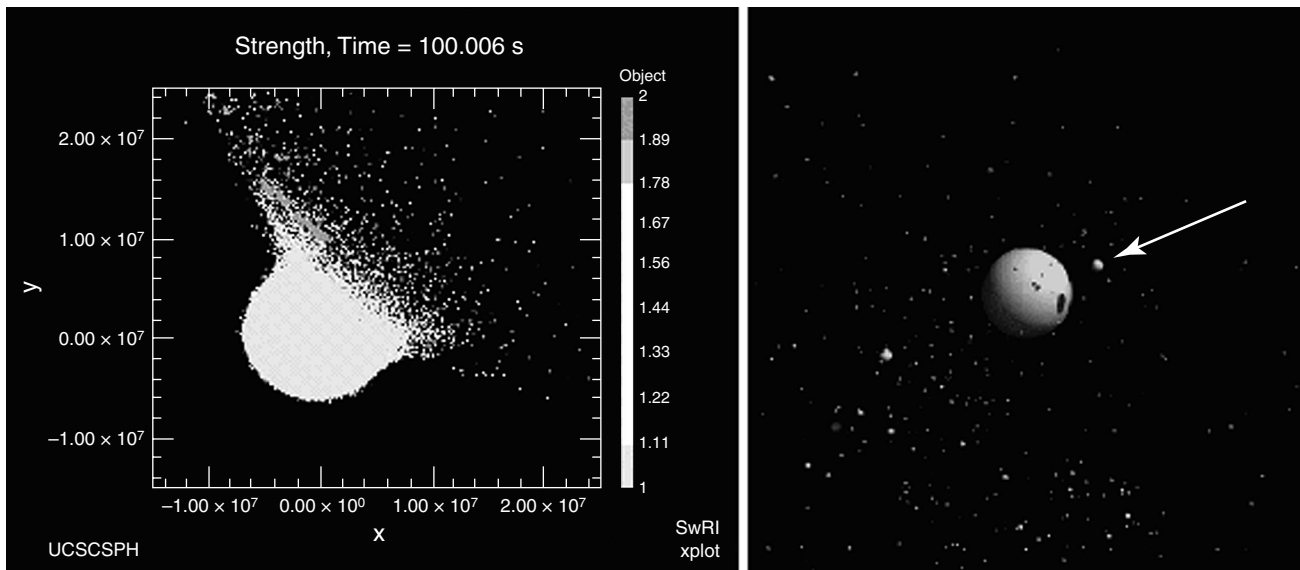
Fig. 11. The "next generation" of numerical models of asteroid satellite formation substantially improve upon past models by (left) conducting detailed three-dimensional smooth-particle hydrodynamics (SPH) models of collisions between asteroids and then (right) following the subsequent dynamics of ejected debris and formation of orbiting satellites (arrow) through fast, state-of-the-art N-body simulations. Shown here is a collision of a 20-km impactor into a 100-km solid basaltic target, as simulated by *Durda et al.* (2001). The ~4-km satellite is captured into an elliptical orbit with a separation of about 6 $R_{primary}$. The final primary diameter is ~75 km.

they would have relative velocities exceeding their mutual escape velocity and in general would not remain gravitationally bound.

This problem was examined in some detail by *Durda* (1996) and by *Doressoundiram et al.* (1997), who simulated disruptions numerically, integrating orbits of fragments in the debris field. They found that the fraction of binaries depends on the magnitude of a random velocity dispersion assumed to be imposed on the general expansion; however, even with no dispersion some binaries were produced, apparently by jostling among fragments. More pairs of fragments in contact were produced than orbiting binaries. The fraction of contact pairs and binaries was small in Durda's models (~0.1%), while the fraction of binaries found by Doressoundiram et al. was ~1%. The limited range of sizes and numbers of particles in the simulations probably limited the binary fraction. Treating larger numbers of smaller fragments would be expected to yield more binaries with smaller satellite:primary mass ratios.

The early, simple numerical models of this mode of satellite formation contained some critical limitations, however. Because the initial conditions simulating the expansion phase following a catastrophic impact were merely treated in a simple empirical fashion, a self-consistent description of the mass-speed distribution of fragments and the direction of fragment ejection was not possible. Variations in these collision outcomes, and therefore in the efficiency of binary-pair formation, with initial conditions, could not be examined in these initial studies. The next generation of numerical models (*Michel et al.,* 2001; *Durda et al.,* 2001) substantially improve upon the limitations of the *Durda* (1996) and *Doressoundiram et al.* (1997) models by conducting detailed three-dimensional smooth-parti-

cle hydrodynamics (SPH) models of catastrophic collisions between asteroids (e.g., *Benz and Asphaug,* 1995; *Asphaug et al.,* 1998) and then following the subsequent dynamics of the ejected fragments through fast, state-of-the-art N-body simulations (such as described in *Leinhardt et al.,* 2000).

One of the most important benefits of this scheme over the previous numerical studies is that it includes a rigorous treatment of the impact physics, so that accurate fragment size distributions and velocity fields are established early in the ejection process. Thus, the dependence of satellite formation efficiency with respect to various collision parameters (e.g., speed, impact parameter, impact angle) can be studied in a self-consistent manner. These new models also allow for a far-faster N-body integration scheme with efficient mutual capture and collision detection capabilities. A sample model can be seen in Fig. 11.

Four of the known main-belt binaries (45, 90, 243, and 3749) are members of dynamical families, so this mechanism is plausible (possibly, the fraction of binaries in families is greater than for the general population). There should be no initial preference for rapid rotation of primaries or prograde orbits, but tidal dissipation could cause loss of satellites of slow rotators or in retrograde orbits. We would expect no correlation with the primary's shape, so light-curves may discriminate between cratering ejecta and disruptive capture.

3.4. Collisional Fission

An impact may shatter an asteroid without disrupting it. As the probability of an exactly central collision is zero, it will also impart angular momentum to the target. If the specific angular momentum exceeds a threshold value, a

weak (shattered) self-gravitating body cannot remain single but must fission into a binary, with some of the angular momentum in orbital motion rather than rotation. The angular momentum imparted is proportional to the impact velocity v, while the impact energy scales as v^2. As discussed by *Weidenschilling et al.* (1989), it is difficult to impart enough angular momentum without destroying the target at typical impact velocities (~5 km s^{-1}) in the present belt (although there is a distribution of velocities over a wide range, but at lower impact probabilities). If gravitational binding dominates, then for impacts large enough to impart the critical angular momentum, the ratio of impact energy to binding energy is of order v_{impact}/v_{escape}. For even the largest asteroids, disruption is more likely than rotational fission in the present collisional environment. Conditions were presumably more favorable in the earliest stage of the belt's evolution, before velocities were pumped up; however, only large satellites would have been able to survive its later collisional history. No convincing candidate systems have yet been found in the main belt.

The masses and relatively large separation (~4 radii) of the main-belt double (90) Antiope imaged by *Merline et al.* (2000a,b) mean that this pair has unusually high specific angular momentum. The lightcurve eclipses recorded by *Hansen et al.* (1997) are consistent with the nearly equal-sized components seen in the images. At other times, the lightcurve had a low amplitude consistent with nearly spherical, noneclipsing components (actually, Darwin ellipsoids are an even better match). *Merline et al.* (2000a,b) inferred a density of ~1.3 g cm^{-3}, which suggests that the Antiope components may be "rubble piles" with equilibrium shapes. Such models of equilibrium binaries and the expected lightcurve morphologies were studied by *Leone et al.* (1984). The origin of the Antiope binary is hard to explain. It is a member of the Themis family and so must postdate the disruption of its parent body by a high-velocity impact. Disruptive capture of two equal-mass fragments of such large size in that event is unlikely, and they would have to be converted to rubble piles by later impacts. However, some of the model runs of P. Michel (personal communication, 2001) appear to produce similar-sized components. Collisional fission seems to be the most likely origin for Antiope, but still presents the problem of imparting so much angular momentum in a collision without dispersing the target. Due to the low orbital inclination of the Themis family, collisions between members have a lower mean velocity [~3 km s^{-1} (*Bottke et al.,* 1994)] than between field asteroids (~5 km s^{-1}) but this difference is not very significant. *Weidenschilling et al.* (2001) estimate that the required angular momentum implies an impactor of diameter ~20 km on a 100-km target body, with about 100 times its gravitational binding energy, at the mean encounter velocity. An impact by a larger body at much lower velocity is improbable, even if the Themis family is several billion years old. Low-velocity impacts could have occurred in the immediate aftermath of the disruption of the Themis family's parent body, before Jovian perturbations randomized the nodes and apsides of the fragments. Models by *Dell'Oro et al.* (2002) show an enhancement in the impact probabilities of several orders of

magnitude initially after breakup. However, the time available before randomization is short (~10^4 orbital periods), and a collision between two fragments of sufficient size is unlikely. In either scenario, the probability of forming a binary with these properties is only ~10^{-3}, and thus Antiope should be unique in the main belt.

3.5. Primordial Binaries?

Other binaries with components of comparable mass and large separations have been discovered, but at larger heliocentric distances. The Trojan asteroid (617) Patroclus (*Merline et al.,* 2001b) and at least two of the TNO binaries (1998 WW$_{31}$, 2001 QW$_{322}$) have size ratios close to one. All have significantly greater separations than Antiope: ~600 km (~12 radii) for Patroclus and 10^4–10^5 km (~10^2–10^3 radii) for the TNOs. In one sense, these properties are not surprising, because detection of smaller and/or closer satellites of such distant objects is impossible with current technology. However, it is unclear how such loosely bound pairs could have formed. If the Patroclus binary formed by a collision, it would have required more extreme parameters (larger impactor and/or lower velocity) than Antiope's formation. The collision rate in the Trojan clouds is somewhat higher than in the main belt (see *Davis et al.,* 2002), while the mean impact velocity is comparable (lower orbital velocity is offset by higher mean inclination). However, a binary of this size would have a collisional lifetime greater than the age of the solar system. It is plausible, therefore, that the Patroclus binary formed by a low-velocity collision before eccentricities and inclinations were pumped up, perhaps before its capture into resonance with Jupiter.

The frequency of transneptunian binaries appears to be ~1%. Their large separations could not have been produced by two-body collisions or tidal evolution. The most plausible origin for such a loosely bound binary seems to be an impact with another body of comparable mass while the two components passed within their mutual Hill radius. The present spatial density in the Kuiper Belt is far too low for three-body encounters; any such events must have occurred when it was more populous and/or dynamically "cold" with low inclinations. Dynamical modeling is needed to determine the efficiency of binary production by this mechanism as a function of population density and orbital parameters. Alternatively, these binaries may represent objects that formed as loosely bound pairs from inherent disk instabilities during accretion (S. A. Stern, personal communication, 2001). Observations of binary TNOs will eventually allow direct determination of their masses and densities, but may also provide a constraint on the formation and early history of the Kuiper Belt.

3.6. Tidal Evolution of Spins and Orbits

Weidenschilling et al. (1989) consider the tidal evolution of orbits of asteroid satellites. Their Fig. 1 shows the timescale for a hypothetical satellite to evolve outward from an orbit initially close to a primary of radius R = 100 km, as a function of the satellite:primary mass ratio. There are

now enough data for real binaries to compare this model with observation. Most of the known main-belt binaries have separations $a/R \sim 10$, and $M/m \sim 3 \times 10^2$–10^4 (Table 2); the inferred tidal evolution timescales are in the range $\sim 10^8$–10^9 yr. These values depend on the mechanical properties of the primaries, which are uncertain, but are consistent with collisional production of close binaries and tidal expansion of their orbits to their present distances since the formation of the asteroid belt. All such satellites lie below the line of synchronous stability, with orbits that are still evolving outward (consistent with the observation that their primaries have rotation periods shorter than their orbital periods). The NEAs typically have smaller separations with $a/R \sim 5$, and smaller $M/m \sim 10^1$–2×10^2. However, they are much smaller than the main-belt binaries, with $R \sim 1$ km; since the rate of tidal evolution of orbits scales as R^2, they also have timescales $\sim 10^9$ yr, consistent with the observation that they have not evolved to a synchronous end state. The binaries with relatively close massive satellites have much shorter evolution times; extrapolating from Weidenschilling et al.'s Fig. 1, (90) Antiope would have reached its tidally locked end state in only a few thousand years, and (617) Patroclus in less than 10^6 yr. However, it can be seen from that figure that Patroclus has too much angular momentum to have evolved by despinning of an initially close binary. This system, and the Kuiper Belt binaries with comparable mass ratios and still larger separations, must have attained their present orbital configurations by a mechanism other than tidal despinning.

The timescale for despinning of a satellite's rotation by tides is generally shorter than that for evolution of its orbit by despinning of the primary. Using the classic formula for the rate of despinning (*Goldreich and Soter,* 1966), the smaller main-belt and NEA satellites have despinning times of $\sim 10^6$–10^7 yr, so they would be expected to keep one face toward their primary. The only observational datum for rotation of a main-belt satellite is from the *Galileo* flyby of Ida/Dactyl, which shows that Dactyl had slow rotation, consistent with spin-orbit synchronicity (*Veverka et al.,* 1996b). On the other hand, the known Kuiper Belt binaries have such large separations that their tidal despinning times probably exceed the age of the solar system; they are unlikely to be in synchronous rotation.

Finally, *Harris* (2002) has suggested that the gravitational ejection of a satellite from orbit around an irregularly shaped primary would deplete the rotational energy of the primary, thus slowing substantially the spin of the primary. This ultimately may be shown to be the cause of the anomalously slow rotation of many asteroids, which so far have eluded satisfactory explanation.

3.7. Triple and Multiple Systems

Little work has been done specifically on the formation and stability of triple or multiple asteroid systems. Perhaps the closest analogs are those studies of the stability of satellites around a nonspherical primary (e.g., *Scheeres,* 1994;

Petit et al., 1997). Significant progress, however, has been made in the understanding of triple- or multiple-star systems. Many of these results can be applied directly to asteroids for insight into what characteristics might be expected for multiple-asteroid systems. It is generally accepted that the masses would be configured in a hierarchical fashion (cf. *Eggleton and Kiseleva,* 1995). This would involve the superposition of two binary systems: an inner massive object orbited by a satellite and a moon of the satellite (like Sun/Earth/Moon) or a close binary system with a tertiary object in a wide orbit about the central pair. The ratio of the semimajor axes of the two relevant "binaries" must be ~ 3–4 to be stable (*Harrington,* 1977a,b). For eccentric orbits, the ratio of the periapse of the outer orbit to the inner semimajor axis is the relevant parameter. Eccentric orbits are therefore less stable (*Eggleton and Kiseleva,* 1995; *Kiseleva et al.,* 1994). In addition, the stability depends, in a complicated way, on the mass ratios of the objects (*Black,* 1982). Systems that have the two orbits counter-revolving (retrograde) also display greater stability than if the orbits are both in the same sense (*Harrington,* 1977b). Recent work on evolution of triple systems (*Miller and Hamilton,* 2002) emphasizes the importance of Kozai resonances in stability and indicates a strong preference that the orbits be approximately coplanar. Multiple systems would be formed in successively higher levels of hierarchy as discussed by *Harrington* (1977b).

Unlike triple-star systems, which can form by gravitational capture, (e.g., during the collision of two binary systems), such a formation mechanism would be difficult for asteroids because of the high encounter velocities relative to the orbital speeds (P. Hut, personal communication, 2002). The initial formation of triple/multiple systems were indicated, however, in the early numerical models of *Durda* (1996) and *Doressoundiram et al.* (1997) and are clearly produced by the next-generation models of *Michel et al.* (2001) and *Durda et al.* (2001). These SPH/N-body models of satellite formation show that in addition to producing binary systems with a single satellite in orbit about a primary asteroid, catastrophic disruption events can result (at least initially) in more complex, hierarchical systems with satellites of satellites. The gravitational reaccumulation of clumps of debris in the ejecta field around the largest remnant often leads to Shoemaker-Levy/9-like "strings-of-pearls." Many of these reaccumulating rubble-pile fragments, some of which are gravitationally bound in initially stable orbits around the largest remnant, are themselves surrounded by swarms of smaller orbiting debris. The simulation timescales are too short, thus far, to directly examine the longer-term stability of these hierarchical satellite systems.

4. SUMMARY

The question posed in the title to the Weidenschilling et al. chapter in *Asteroids II*, "Do Asteroids Have Satellites?," has now been answered. Now that we have many examples of binary systems for study, representing diverse collisional

and dynamical populations, we may be at the threshold of a revolution in asteroid science. In the *next* decade, we can expect to learn a great deal from the ever-increasing pace of discovery, involving several rapidly improving, complementary techniques, as well as the concomitant numerical modeling and theoretical thinking about how these systems were formed, how they evolve, and what clues they hold to the history of the solar system. These binary systems will provide probes of asteroid interiors and perhaps will eventually allow definitive coupling of asteroid taxonomic type with the meteorite inventory. In fact, they may tell us about asteroid material for which it is unlikely we currently have representation among the meteorites, such as very low-density carbonaceous material that may not survive passage through Earth's atmosphere or primitive material of the outer main-belt, Trojan, or TNO regions. Research in this area will lead to spinoffs in related areas, including improvements to our understanding of the formation of the Earth/Moon or Pluto/Charon systems, dynamics and collisional physics, and assist in the mitigation of impact hazards to Earth.

REFERENCES

André C. (1901) Sur le système formé par la planète double (433) Eros. *Astron. Nachr., 155,* 27–30.

Asphaug E., Moore J. M., Morrison D., Benz W., Nolan M. C., and Sullivan R. J. (1996) Mechanical and geological effects of impact cratering on Ida. *Icarus, 120,* 158–184.

Asphaug E., Ostro S. J., Hudson R. S., Scheeres D. J., and Benz W. (1998) Disruption of kilometre-sized asteroids by energetic collisions. *Nature, 393,* 437–440.

Belton M. and Carlson R. (1994) *1993 (243) 1.* IAU Circular No. 5948.

Belton M. J. S., Veverka J., Thomas P., Helfenstein P., Simonelli D., Chapman C., Davies M. E., Greeley R., Greenberg R., Head J., Murchie S., Klaasen K., Johnson T. V., McEwen A., Morrison D., Neukum G., Fanale F., Anger C., Carr M., and Pilcher C. (1992) *Galileo* encounter with 951 Gaspra: First pictures of an asteroid. *Science, 257,* 1647–1652.

Belton M. J. S., Chapman C. R., Thomas P. C., Davies M. E., Greenberg R., Klaasen K., Byrnes D., D'Amario L., Synnott S., Johnson T. V., McEwen A., Merline W. J., Davis D., Petit J-M., Storrs A., Veverka J., and Zellner B. (1995) Bulk density of asteroid 243 Ida from the orbit of its satellite Dactyl. *Nature, 374,* 785–788.

Belton M. J. S., Mueller B. E. A., D'Amario L., Byrnes D. V., Klaasen K. P., Synnott S., Breneman H., Johnson T. V., Thomas P. C., Veverka J., Harch A. C., Davies M. E., Merline W. J., Chapman C. R., Davis D. R., Denk T., Petit J-M., Greenberg R., Storrs A., and Zellner B. (1996) The discovery and orbit of 1993 (243) 1 Dactyl. *Icarus, 120,* 185–199.

Benner L. A. M., Ostro S. J., Giorgini J. D., Jurgens R. F., Margot J.-L., and Nolan M. C. (2001a) *1999 KW$_4$.* IAU Circular No. 7632.

Benner L. A. M., Nolan M. C., Ostro S. J., Giorgini J. D., and Margot J.-L. (2001b) *1998 ST$_{27}$.* IAU Circular No. 7730.

Benz W. and Asphaug E. (1995) Simulations of brittle solids using smooth particle hydrodynamics. *Comput. Phys. Commun., 87,* 253–265.

Binzel R. P. (1998) Collisional evolution in the Eros and Koronis asteroid families: Observational and numerical results. *Icarus, 73,* 303–313.

Binzel R. P., Gaffey M. J., Thomas P. C., Zellner B. H., Storrs A. D., and Wells E. N. (1997) Geologic mapping of Vesta from 1994 Hubble Space Telescope images. *Icarus, 128,* 95–103.

Black D. C. (1982) A simple criterion for determining the dynamical stability of three-body systems. *Astron. J., 87,* 1333–1337.

Bottke W. F. Jr. and Melosh H. J. (1996a) The formation of asteroid satellites and doublet craters by planetary tidal forces. *Nature, 381,* 51–53.

Bottke W. F. Jr. and Melosh H. J. (1996b) The formation of binary asteroids and doublet craters. *Icarus, 124,* 372–391.

Bottke W. F., Nolan M., and Greenberg R. (1994) Velocity distributions among colliding asteroids. *Icarus, 107,* 255–268.

Bottke W. F. Jr., Richardson D. C., Michel P., and Love S. G. (1999) 1620 Geographos and 433 Eros: Shaped by planetary tides? *Astron. J., 117,* 1921–1928.

Britt D. T. and Consolmagno G. J. (2000) The porosity of dark meteorites and the structure of low-albedo asteroids. *Icarus, 146,* 213–219.

Britt D. T. and Consolmagno G. J. (2001) Modeling the structure of high porosity asteroids. *Icarus, 152,* 134–139.

Brown M. E. and Margot J.-L. (2001) *S/2001 (87) 1.* IAU Circular No. 7588.

Brown M. E. and Trujillo C. A. (2002) (26308) *1998 SM$_{165}$.* IAU Circular No. 7807.

Cellino A., Pannunzio R., Zappalà V., Farinella P., and Paolicchi P. (1985) Do we observe light curves of binary asteroids? *Astron. Astrophys., 144,* 355–362.

Chapman C. R. (1996) S-type asteroids, ordinary chondrites, and space weathering: The evidence from *Galileo*'s fly-bys of Gaspra and Ida. *Meteoritics & Planet Sci., 31,* 699–726.

Chapman C. R. (2002) Cratering on asteroids from *Galileo* and *NEAR Shoemaker*. In *Asteroids III* (W. F. Bottke Jr. et al., eds.), this volume. Univ. of Arizona, Tucson.

Chapman C. R., Veverka J., Thomas P. C., Klaasen K., Belton M. J. S., Harch A., McEwen A., Johnson T. V., Helfenstein P., Davies M. E., Merline W. J., and Denk T. (1995) Discovery and physical properties of Dactyl, a satellite of asteroid 243 Ida. *Nature, 374,* 783–785.

Chapman C. R., Ryan E. V., Merline W. J., Neukum G., Wagner R., Thomas P. C., Veverka J., and Sullivan R. J. (1996) Cratering on Ida. *Icarus, 120,* 77–86.

Chauvineau B. and Mignard F. (1990) Dynamics binary asteroids II. Jovian perturbations. *Icarus, 87,* 377–390.

Chauvineau B., Farinella P., and Mignard F. (1993) Planar orbits about a triaxial body: Applications to asteroidal satellites. *Icarus, 105,* 370–384.

Cheng A. F. (2002) Near-Earth asteroid rendezvous: Mission summary. In *Asteroids III* (W. F. Bottke Jr. et al., eds.), this volume. Univ. of Arizona, Tucson.

Close L. M., Merline W. J., Tholen D. J., Owen T. C., Roddier F., and Dumas C. (2000) Adaptive optics imaging of Pluto-Charon and the discovery of a moon around the asteroid 45 Eugenia: The potential of adaptive optics in planetary astronomy. *Proc. SPIE 4007,* pp. 787–795.

Davis D. R., Chapman C. R., Durda D. D., Farinella P., and Marzari F. (1996) The formation and collisional/dynamical evolution of the Ida/Dactyl system as part of the Koronis family. *Icarus, 120,* 220–230.

Davis D. R., Durda D. D., Marzari F., Campo Bagatin A., and Gil-Hutton R. (2002) Collisional evolution of small-body pop-

ulations. In *Asteroids III* (W. F. Bottke Jr. et al., eds.), this volume. Univ. of Arizona, Tucson.

Davis R. G. (2001) High precision lightcurves for 762 Pulcova. *Minor Planet Bull., 28,* 10–12.

Dell'Oro A., Paolicchi P., Cellino A., and Zappalà V. (2002) Collisional rates within newly formed asteroid families. *Icarus, 156,* 191–201.

Doressoundiram A., Paolicchi P., Verlicchi A., and Cellino A. (1997) The formation of binary asteroids as outcomes of catastrophic collisions. *Planet. Space. Sci., 45,* 757–770.

Dotto E., Barucci M. A., Müller T. G., Storrs A. D., and Tanga P. (2002) Observations from orbiting platforms. In *Asteroids III* (W. F. Bottke Jr. et al., eds.), this volume. Univ. of Arizona, Tucson.

Durda D. D. (1996) The formation of asteroidal satellites in catastrophic collisions. *Icarus, 120,* 212–219.

Durda D. D. and Geissler P. (1996) The formation of asteroidal satellites in large cratering collisions. *Bull. Am. Astron. Soc., 28,* 1101.

Durda D. D., Bottke W. F., Asphaug E., and Richardson D. C. (2001) The formation of asteroid satellites: Numerical simulations using SPH and N-body models. *Bull. Am. Astron. Soc., 33,* 5203.

Eggleton P. and Kiseleva L. (1995) An empirical condition for stability of hierarchical triple systems. *Astrophys. J., 455,* 640–645.

Elliot J. L., Kern S. D., Osip D. J., and Burles S. M. (2001) *2001 QT$_{297}$.* IAU Circular No. 7733.

Gehrels T., Drummond J. D., and Levenson N. A. (1987) The absence of satellites of asteroids. *Icarus, 70,* 257–263.

Geissler P., Petit J.-M., Durda D. D., Greenberg R., Bottke W., Nolan M., and Moore J. (1996) Erosion and ejecta reaccretion on 243 Ida and its moon. *Icarus, 120,* 140–157.

Goldreich P. and S. Soter (1996) Q in the solar system. *Icarus, 5,* 375–389.

Gradie J. and Flynn L. (1998) A search for satellites and dust belts around asteroids: Negative results (abstract). In *Lunar and Planetary Science XIX,* pp. 405–406. Lunar and Planetary Institute, Houston.

Graves J. E., Northcott M. J., Roddier F. J., Roddier C. A., and Close L. M. (1998) First light for Hokupa'a: 36-element curvature AO system at UH. *Proc. SPIE 3353,* pp. 34–43.

Hamilton D. P. and Burns J. A. (1991) Orbital stability zones about asteroids. *Icarus, 92,* 118–131.

Hansen A. T., Arentoft T., and Lang K. (1997) The rotational period of 90 Antiope. *Minor Planet Bull., 24,* 17.

Harrington R. S. (1997a) Planetary orbits in binary stars. *Astron. J., 82,* 753–756.

Harrington R. S. (1997b) A review of the dynamics of classical triple stars. *Rev. Mex. Astron. Astrofis., 3,* 139–143.

Harris A. W. (2002) On the slow rotation of asteroids. *Icarus, 156,* 184–190.

Harris A. W. and Davies J. K. (1999) Physical characteristics of near-Earth asteroids from thermal infrared spectrophotometry. *Icarus, 142,* 464–475.

Hartmann W. K. (1979) Diverse puzzling asteroids and a possible unified explanation. In *Asteroids* (T. Gehrels, ed.), pp. 466–479. Univ. of Arizona, Tucson.

Hudson R. S. (1993) Three-dimensional reconstruction of asteroids from radar observations. *Remote Sensing Rev., 8,* 195–203.

Hudson R. S. and Ostro S. J. (1994) Shape of asteroid 4769 Castalia (1989 PB) from inversion of radar images. *Science, 263,* 940–943.

Kaasalainen M., Mottola S., and Fulchignoni M. (2002) Asteroid models from disk-integrated data. In *Asteroids III* (W. F. Bottke Jr. et al., eds.), this volume. Univ. of Arizona, Tucson.

Kavelaars J. J., Petit J.-M., Gladman B., and Holman M. (2001) *2001 QW$_{322}$.* IAU Circular No. 7749.

Kiseleva L., Eggleton P. P., and Orlov V. V. (1994) Instability of close triple systems with coplanar initial doubly circular motion. *Mon. Not. R. Astron. Soc., 270,* 936–946.

Leinhardt Z. M., Richardson D. C., and Quinn T. (2000) Direct N-body simulations of rubble pile collisions. *Icarus, 146,* 133–151.

Leone G., Farinella P., Paolicchi P., and Zappalà V. (1984) Equilibrium models of binary asteroids. *Astron. Astrophys. 140,* 265–272.

Love S. G. and Ahrens T. J. (1997) Origin of asteroid rotation rates in catastrophic impacts. *Nature, 386,* 154–156.

Margot J.-L. and Brown M. E. (2001) *S/2001 (22) 1.* IAU Circular No. 7703.

Margot J.-L., Nolan M. C., Benner L. A. M., Ostro S. J., Jurgens R. F., Slade M. A., Giorgini J. D., and Campbell D. B. (2000) *Satellites of Minor Planets.* IAU Circular No. 7503.

Margot J.-L., Nolan M. C., Benner L. A. M., Ostro S. J., Jurgens R. F., Giorgini J. D., Slade M. A., Howell E. S., and Campbell D. B. (2002a) Radar discovery and characterization of binary near-Earth asteroids (abstract). In *Lunar and Planetary Science XXXIII,* Abstract #1849. Lunar and Planetary Institute, Houston (CD-ROM).

Margot J.-L., Nolan M. C., Benner L. A. M., Ostro S. J., Jurgens R. F., Giorgini J. D., Slade M. A., and Campbell D. B. (2002b) Binary asteroids in the near-Earth object population. *Science, 296,* 1445–1448.

Merline W. J., Chapman C. R., Robinson M., Veverka J., Harch A., Bell J. III, Thomas P., Clark B. E., Joseph J., Carcich B, Murchie S., Cheng A., Izenberg N., McFadden L., and Malin M. (1998) *NEAR*'s encounter with 253 Mathilde: Search for satellites (abstract). In *Lunar and Planetary Science XXIX,* Abstract #1954. Lunar and Planetary Institute, Houston (CD-ROM).

Merline W. J., Chapman C. R., Colwell W. B., Veverka J., Harch A., Bell M., Bell J. III, Thomas P., Clark B. E., Martin P., Murchie S., Cheng A., Domingue D., Izenberg N., Robinson M., McFadden L., Wellnitz D., Malin M., Owen W., and Miller J. (1999a) Search for satellites around asteroid 433 Eros from *NEAR* flyby imaging (abstract). In *Lunar and Planetary Science XXX,* Abstract #2055. Lunar and Planetary Institute, Houston (CD-ROM).

Merline W. J., Close L. M., Dumas C., Chapman C. R., Roddier F., Ménard F., Slater D. C., Duvert G., Shelton C., Morgan T., and Dunham D. W. (1999b) *S/1998 (45) 1.* IAU Circular No. 7129.

Merline W. J., Close L. M., Dumas C., Chapman C. R., Roddier F., Ménard F., Slater D. C., Duvert G., Shelton C., and Morgan T. (1999c) Discovery of a moon orbiting the asteroid 45 Eugenia. *Nature, 401,* 565–568.

Merline W. J., Close L. M., Dumas C., Shelton J. C., Ménard F., Chapman C. R., and Slater D. C. (2000a) *Satellites of Minor Planets.* IAU Circular No. 7503.

Merline W. J., Close L. M, Dumas C., Shelton J. C., Ménard F., Chapman C. R., and Slater D. C. (2000b) Discovery of companions to asteroids 762 Pulcova and 90 Antiope by direct im-

aging. *Bull. Am. Astron. Soc., 32,* 1309.

Merline W. J., Ménard F., Close L., Dumas C., Chapman C. R., and Slater D. C. (2001a) *S/2001 (22) 1.* IAU Circular No. 7703.

Merline W. J., Close L. M., Siegler N., Potter D., Chapman C. R., Dumas C., Ménard F., Slater D. C., Baker A. C., Edmunds M. G., Mathlin G., Guyon O., and Roth K. (2001b) *S/2001 (617) 1.* IAU Circular No. 7741.

Merline W. J., Tamblyn P., Chapman C. R., Colwell W. B., Gor V., Burl M. C., Bierhaus E. B., and Robinson M. S. (2001c) An automated search for moons during approach of the *NEAR* spacecraft to asteroid Eros. *Proc. 6th International Symposium on Artificial Intelligence, Robotics, and Automation in Space, 2001 (Montreal),* Paper #AM128 (CD-ROM).

Merline W. J., Close L. M., Mènard F., Dumas C., Chapman C. R., Slater D. C. (2001d) Search for asteroidal satellites. *Bull. Am. Astron. Soc., 32,* 1017.

Merline W. J., Close L. M., Siegler N., Dumas C., Chapman C., Rigaut F., Ménard F., Owen W. M., and Slater D. C. (2002) *S/2002 (3749) 1.* IAU Circular No. 7827.

Michel P., Benz W., Tanga P., Richardson D. C. (2001) Collisions and gravitational re-accumulation: Forming asteroid families and satellites. *Science, 294,* 1696–1700.

Miller M. C. and Hamilton D. P. (2002) Four-body effects in globular cluster black hole coalescence. *Astrophys. J., 576,* 894–898.

Mottola S. and Lahulla F. (2000) Mutual eclipse events in asteroidal binary system 1996 FG$_3$: Observations and a numerical model. *Icarus, 146,* 556–567.

Mottola S., De Angelis G., Di Martino M., Erikson A., Hahn G., and Neukum G. (1995) The near-Earth objects follow-up program: First results. *Icarus, 117,* 62–70.

Mottola S., Hahn G., Pravec P., and Šarounová L. (1997) *S/1997 (3671) 1.* IAU Circular No. 6680.

Nolan M. C., Margot J.-L., Howell E. S., Benner L. A. M., Ostro S. J., Jurgens R. F., Giorgini J. D., and Campbell D. B. (2000) *2000 UG$_{11}$.* IAU Circular No. 7518.

Nolan M. C., Howell E. S., Magri C., Beeney B., Campbell D. B., Benner L. A. M., Ostro S. J., Giorgini J. D., and Margot J-L. (2002a) *2002 BM$_{26}$.* IAU Circular No. 7824.

Nolan M. C., Howell E. S., Ostro S. J., Benner L. A. M., Giorgini J. D., Margot J. L., and Campbell D. B. (2002b) *2002 KK$_8$.* IAU Circular No. 7921.

Noll K., Stephens D., Grundy W., Spencer J., Millis R., Buie M., Cruikshank D., Tegler S., and Romanishin W. (2002a) *1997 CQ$_{29}$.* IAU Circular No. 7824.

Noll K., Stephens D., Grundy W., Spencer J., Millis R., Buie M., Cruikshank D., Tegler S., Romanishin W. (2002b) *2000 CF$_{105}$.* IAU Circular No. 7857.

Ostro S. J., Chandler J. F., Hine A. A., Rosema K. D., Shapiro I. I., and Yeomans D. K. (1990) Radar images of asteroid (1990) 1989 PB. *Science, 248,* 1523–1528.

Ostro S. J., Hudson R. S., Nolan M. C., Margot J-L., Scheeres D. J., Campbell D. B., Margi C., Giorgini J. D., and Yeomans D. K. (2000a) Radar observations of asteroid 216 Kleopatra. *Science, 288,* 836–839.

Ostro S. J., Margot J.-L., Nolan M. C., Benner L. A. M., Jurgens R. F., and Giorgini J. D. (2000b) *2000 DP$_{107}$.* IAU Circular No. 7496.

Ostro S. J., Hudson R. S., Benner L. A. M., Giorgini J. D., Magri C., Margot J.-L., and Nolan M. C. (2002) Asteroid radar astronomy. In *Asteroids III* (W. F. Bottke Jr. et al., eds.), this volume. Univ. of Arizona, Tucson.

Paolicchi P., Burns J. A., and Weidenschilling S. J. (2002) Side effects of collisions: Rotational properties and tumbling and binary asteroids. In *Asteroids III* (W. F. Bottke Jr. et al., eds.), this volume. Univ. of Arizona, Tucson.

Petit J.-M., Durda D. D., Greenberg R., Hurford T. A., and Geissler P. E. (1997) The long-term stability of Dactyl's orbit. *Icarus, 130,* 177–197.

Pravec P. (1995) Rotation studies and orbital distribution of near-Earth asteroids. Ph.D. thesis, Charles University, Prague.

Pravec P. and Hahn G. (1997) Two-period lightcurve of 1994 AW$_1$: Indication of a binary asteroid? *Icarus, 127,* 431–440.

Pravec P. and Harris A. W. (2000) Fast and slow rotation of asteroids. *Icarus, 148,* 12–20.

Pravec P. and Šarounová L. (2001) *1999 KW$_4$.* IAU Circular No. 7633.

Pravec P., Wolf M., Varady M., and Bárta P. (1995) CCD photometry of 6 near-Earth asteroids. *Earth Moon Planets, 71,* 177–187.

Pravec P., Wolf M., Šarounová L. (1998a) Occultation/eclipse events in binary asteroid 1991 VH. *Icarus, 133,* 79–88.

Pravec P., Šarounová L., and Wolf M. (1998b) *1996 FG$_3$.* IAU Circular No. 7074.

Pravec P., Wolf M., Šarounová L. (1999) How many binaries are there among near-Earth asteroids? In *Evolution and Source Regions of Asteroids and Comets* (J. Svoreò et al., eds.), pp. 159–162. IAU Colloquium No. 173, Astron. Inst. Slovak Acad. Sci., Tatranská Lomnica.

Pravec P., Šarounová L., Rabinowitz D. L., Hicks M. D., Wolf M., Krugly Y. N., Velichko F. P., Shevchenko V. G., Chiorny V. G., Gaftonyuk N. M., and Genevier G. (2000a) Two-period lightcurves of 1996 FG$_3$, 1998 PG, and (5407) 1992 AX: One probable and two possible binary asteroids. *Icarus, 146,* 190–203.

Pravec P., Kušnirák P., Hicks M., Holliday B., and Warner B. (2000b) *2000 DP$_{107}$.* IAU Circular No. 7504.

Pravec P., Kušnirák P., and Warner B. (2001) *2001 SL$_9$.* IAU Circular No. 7742.

Pravec P., Šarounová L., Hicks M. D., Rabinowitz D. L., Wolf M., Scheirich P., Krugly Y. N. (2002a) Two periods of 1999 HF$_1$ — another binary NEA candidate. *Icarus, 158,* 276–280.

Pravec P., Harris A. W., and Michałowski T. (2002b) Asteroid rotations. In *Asteroids III* (W. F. Bottke Jr. et al., eds.), this volume. Univ. of Arizona, Tucson.

Reitsema H. J. (1979) The reliability of minor planet satellite observations. *Science, 205,* 185–186.

Richardson D. C., Bottke W., and Love S. G. (1998) Tidal distortion and disruption of Earth-crossing asteroids. *Icarus, 134,* 47–76.

Rigaut F., Salmon D., Arsenault R., Thomas J., Lai O., Rouan D., Véran J. P., Gigan P., Crampton D., Fletcher J. M., Stilburn J., Boyer C., and Jagourel P. (1998) Performance of the Canada-France-Hawaii Telescope adaptive optics bonnette. *Publ. Astron. Soc. Pacific, 110,* 152–164.

Roberts L. C. Jr., McAlister H. A., and Hartkopf W. I. (1995) A speckle interferometric survey for asteroid duplicity. *Astron. J., 110,* 2463–2468.

Roddier F. (1988) Curvature sensing and compensation: A new concept in adaptive optics. *Appl. Optics, 27,* 1223–1225.

Roddier F., Northcott, M. and Graves J. E. (1991) A simple low-order adaptive optics system for near infrared applications. *Publ. Astron. Soc. Pac., 103,* 131–149.

Scheeres D. J. (1994) Dynamics about uniformly rotating tri-axial

ellipsoids. *Icarus, 110,* 225–238.

Scheeres D. J., Durda D. D., and Geissler P. E. (2002) The fate of asteroid ejecta. In *Asteroids III* (W. F. Bottke Jr. et al., eds.), this volume. Univ. of Arizona, Tucson.

Showalter M. R., Ostro S. J., Shapiro I. I., and Campbell D. B. (1982) Upper limit on the radar cross section of a Pallas satellite. *Bull. Am. Astron. Soc., 14,* 725.

Storrs A., Wells E., Stern A., and Zellner B. (1998) Surface heterogeneity of asteroids: HST WFPC2 images 1996–1997. *Bull. Am. Astron. Soc., 30,* 1026.

Storrs A., Weiss B., Zellner B., Burleson W., Sichitiu R., Wells E., Kowal C., and Tholen D. (1999a) Imaging observations of asteroids with Hubble Space Telescope. *Icarus, 137,* 260–268.

Storrs A. D., Wells E. N., Zellner B. H., Stern A., and Durda D. (1999b) Imaging observations of asteroids with HST. *Bull. Am. Astron. Soc., 31,* 1089.

Storrs A., Vilas F., Landis R., Wells E., Woods C., Zellner B., and Gaffey M. (2001a) *S/2001 (107) 1.* IAU Circular No. 7599.

Storrs A., Vilas F., Landis R., Wells, E., Woods C., Zellner B., and Gaffey M. (2001b) *S/2001 (87) 1.* IAU Circular No. 7590.

Tanga P., Hestroffer D., Berthier J., Cellino A., Lattanzi M. G., Di Martino M., and Zappalà V. (2001) HST/FGS observations of asteroid (216) Kleopatra. *Icarus, 153,* 451–454.

Toth I. (1999) On the detectability of satellites of small bodies orbiting the Sun in the inner region of the Edgeworth-Kuiper Belt. *Icarus, 141,* 420–425.

Trujillo C. A. and Brown M. E. (2002) *1999 TC$_{36}$.* IAU Circular No. 7787.

Van Flandern T. C., Tedesco E. F. and Binzel R. P. (1979) Satellites of asteroids. In *Asteroids* (T. Gehrels, ed.), pp. 443–465. Univ. of Arizona, Tucson.

Veillet C., Doressoundiram A., Shapiro J., Kavelaars J. J., and Morbidelli A. (2001) *S/2000 (1998 WW$_{31}$) 1.* IAU Circular No. 7610.

Veillet C., Parker J. W., Griffin I., Marsden B., Doressoundiram A., Buie M., Tholen D. J., Connelley M., and Holman M. J. (2002) The binary Kuiper-belt object 1998 WW$_{31}$. *Nature, 416,* 711–713.

Veverka J., Helfenstein P., Lee P., Thomas P., McEwen A., Belton M., Klaasen K., Johnson T. V., Granahan J., Fanale F., Geissler P., and Head J. W. Jr. (1996a) Ida and Dactyl: Spectral reflectance and color variations. *Icarus, 120,* 66–76.

Veverka J., Thomas P. C., Helfenstein P., Lee P., Harch A., Calvo S., Chapman C., Belton M. J. S., Klaasen K., Johnson T. V., and Davies M. (1996b) Dactyl: *Galileo* observations of Ida's satellite. *Icarus, 120,* 200–211.

Veverka J., Thomas P., Harch A., Clark B., Bell J. F. III, Carcich B., Joseph J., Murchie S., Izenberg N., Chapman C., Merline W., Malin M., McFadden L., and Robinson M. (1999a) *NEAR* encounter with asteroid 253 Mathilde: Overview. *Icarus, 140,* 3–16.

Veverka J., Thomas P. C., Bell J. F.III, Bell M., Carcich B., Clark B., Harch A., Joseph J., Martin P., Robinson M., Murchie S., Izenberg N., Hawkins E., Warren J., Farquhar R., Cheng A., Dunham D., Chapman C., Merline W. J., McFadden L., Wellnitz D., Malin M., Owen W. M. Jr., Miller J. K., Williams B. G., and Yeomans D. K. (1999b) Imaging of asteroid 433 Eros during *NEAR*'s flyby reconnaissance. *Science, 285,* 562–564.

Veverka J., Robinson M., Thomas P., Murchie S., Bell J. F. III, Izenberg N., Chapman C., Harch A., Bell M., Carcich B., Cheng A., Clark B., Domingue D., Dunham D., Farquhar R., Gaffey M. J., Hawkins E., Joseph J., Kirk R., Li H., Lucey P., Malin M., Martin P., McFadden L., Merline W. J., Miller J. K., Owen W. M. Jr., Peterson C., Prockter L., Warren J., Wellnitz D., Williams B. G., and Yeomans D. K. (2000) *NEAR* at Eros: Imaging and spectral results. *Science, 289,* 2088–2097.

Weidenschilling S. J., Paolicchi P. and Zappalà V. (1989) Do asteroids have satellites? In *Asteroids II* (R. P. Binzel et al., eds.), pp. 643–658. Univ. of Arizona, Tucson.

Weidenschilling S. J., Marzari F., Davis D. R., and Neese C. (2001) Origin of the double asteroid 90 Antiope: A continuing puzzle (abstract). In *Lunar and Planetary Science XXXII,* Abstract #1890. Lunar and Planetary Institute, Houston (CD-ROM).

Wizinowich P. L., Acton D. S., Lai O., Gathright J., Lupton W., and Stomski P. J. (2000) Performance of the W. M. Keck Observatory natural guide star adaptive optic facility: The first year at the telescope. *Proc. SPIE 4007,* pp. 2–13.

Zellner B., Wells E. N., Chapman C. R., and Cruikshank D. P. (1989) Asteroid observations with the Hubble Space Telescope and the Space Infrared Telescope Facility. In *Asteroids II* (R. P. Binzel et al., eds.), pp. 949–969. Univ. of Arizona, Tucson.